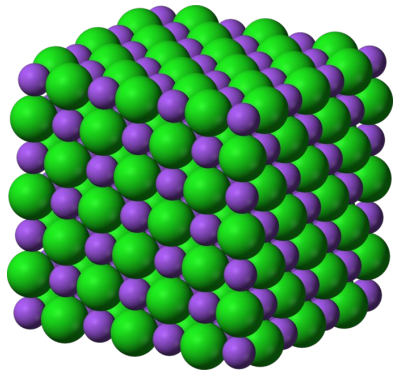


Atomistic modeling of materials for energy storage

Dmitry Aksyonov
Center for Energy Science and Technology, Skoltech



Outline

- 1. Motivation to study energy materials and introduction into battery components*
- 2. Modeling of electrode materials*
- 3. Modeling of electrolytes and interfaces*
- 4. Few examples from our experience: OH defects in LiFePO_4 and antisite defects in layered oxides*

More than 1 billion gasoline cars on Earth



Solution: renewables and electric cars

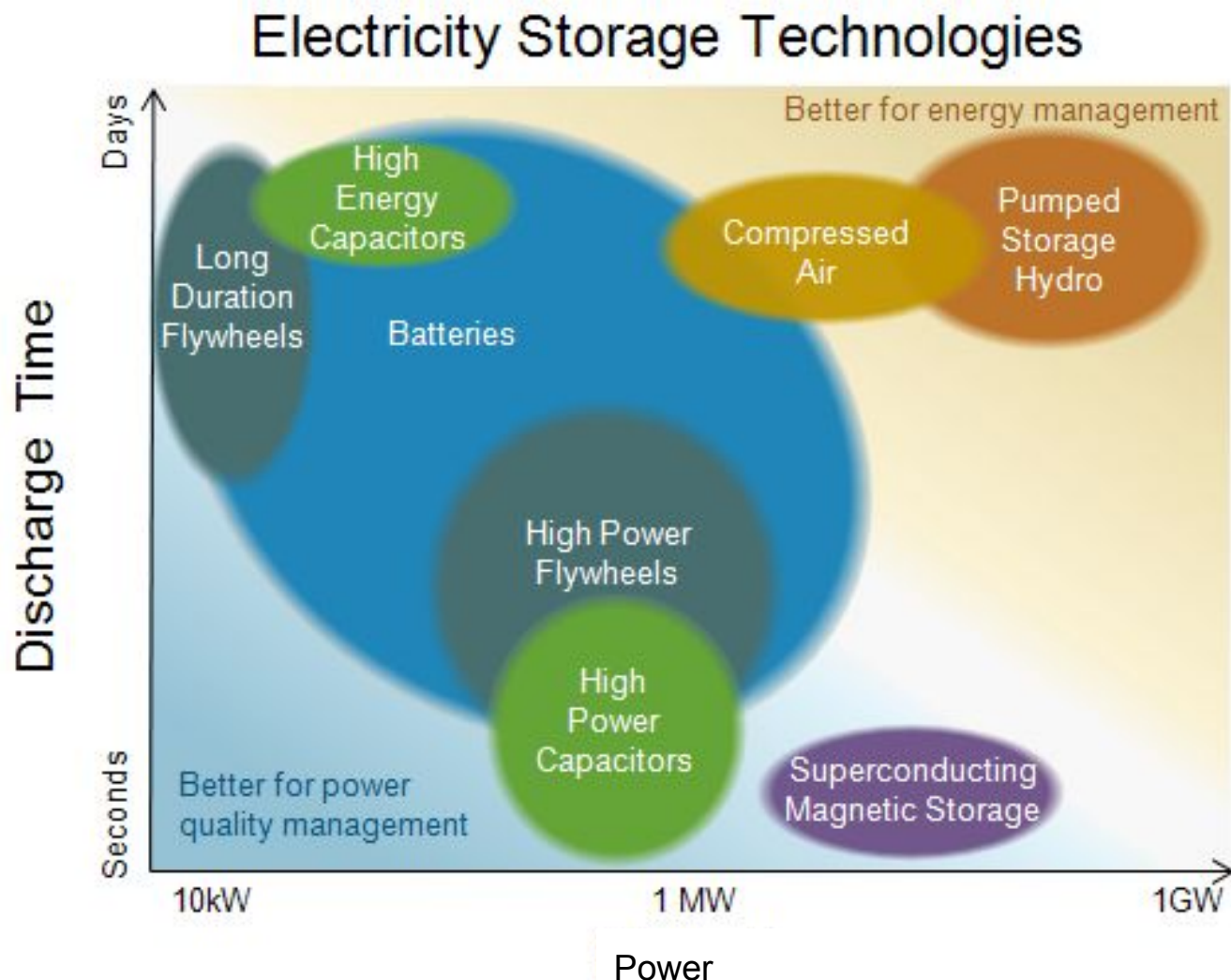
- Renewable electricity is unpredictable
- Electric cars - the range is limited - the price is high
- Both currently are economically unreasonable

What can change the situation?



Affordable energy storage!

Energy storage technologies



Among battery technologies **Li-ion** is the main for portable electronics, cars, and even grid storage

One of the main promoter and adopter of Li-ion technology for heavy energy is Tesla



Model 3/Y 2 mln in 2024



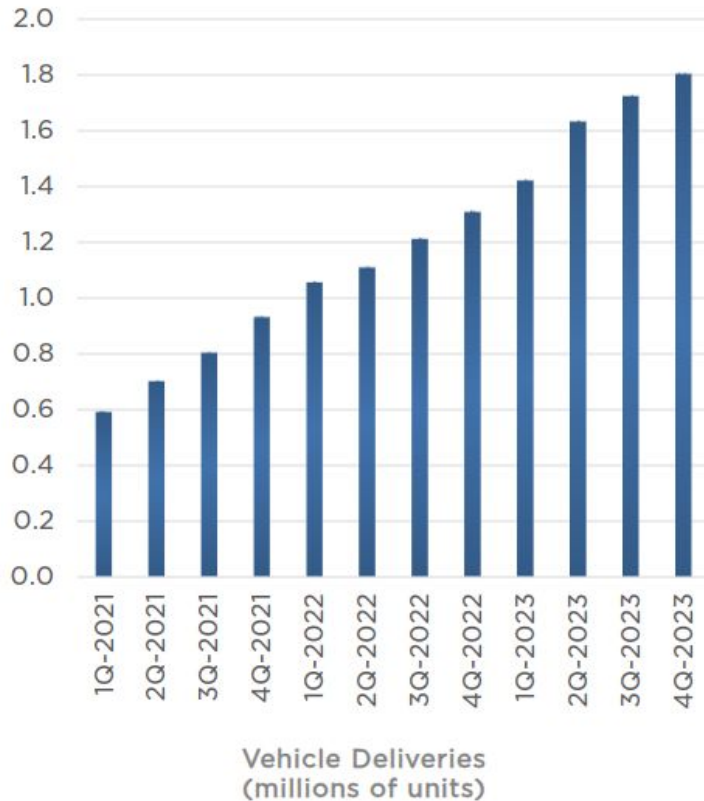
Tesla heavy Truck



Tesla Solar+Storage

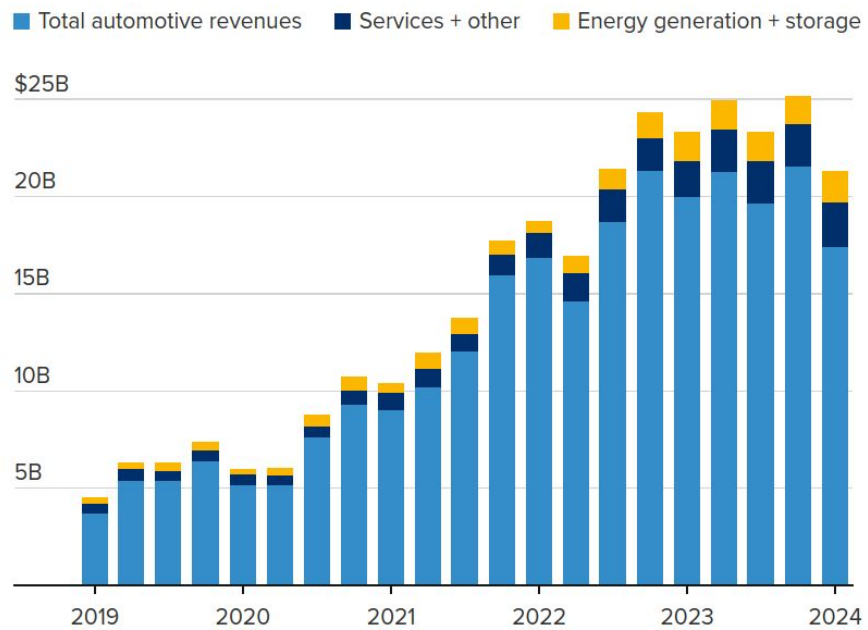


Tesla car production and revenues

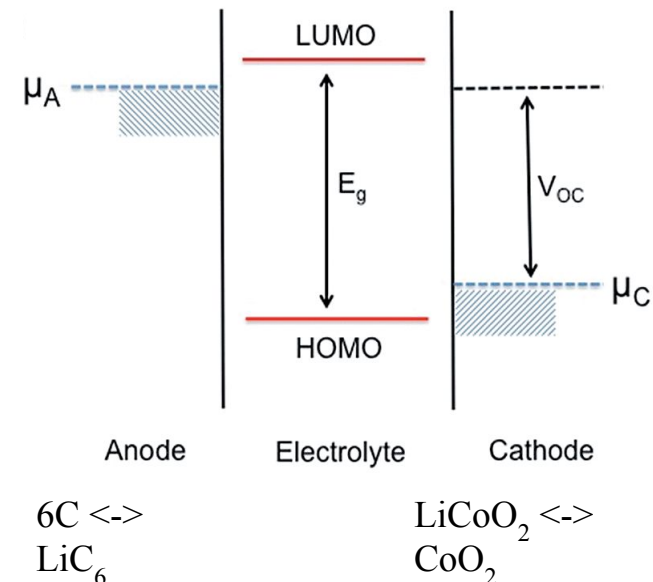
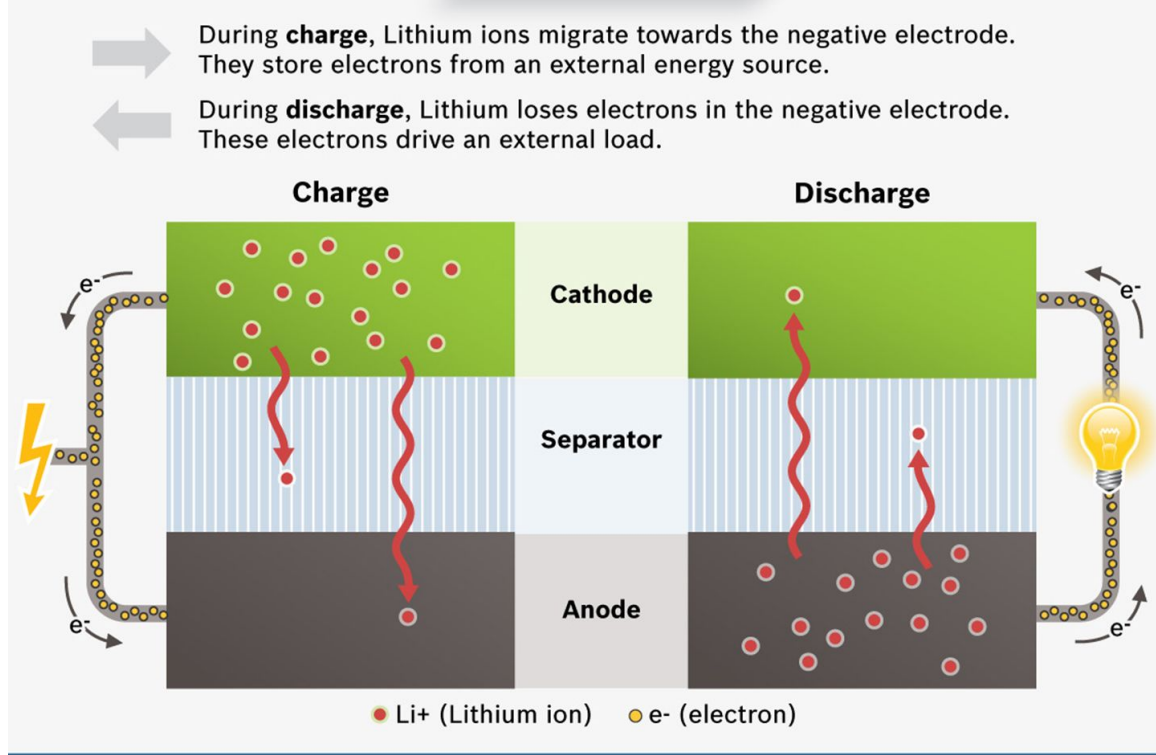
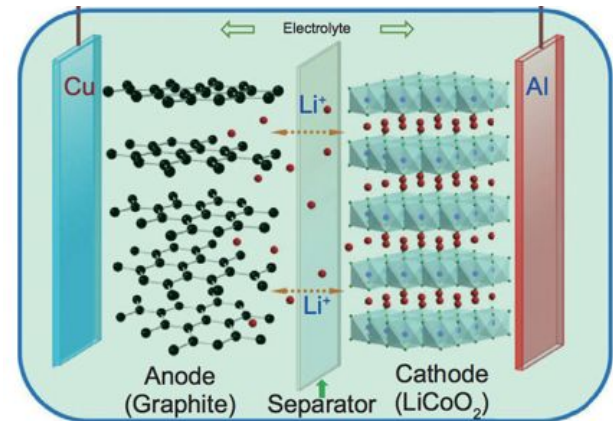
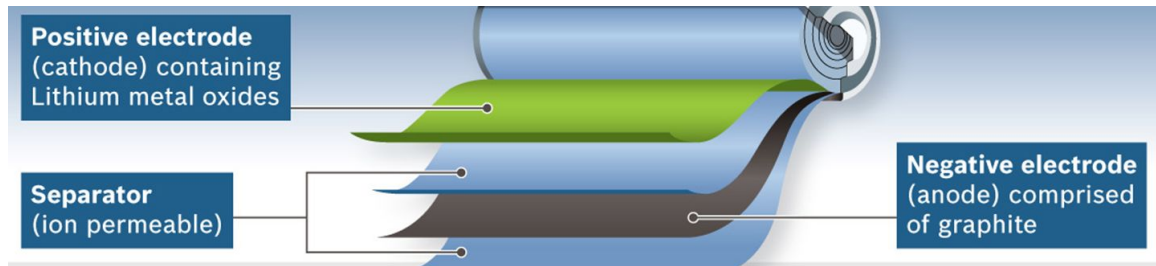


Tesla quarterly revenues

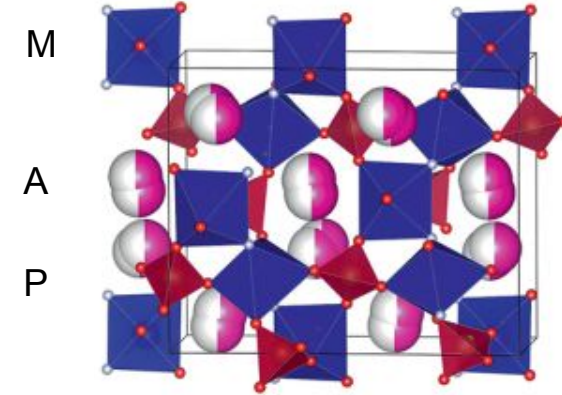
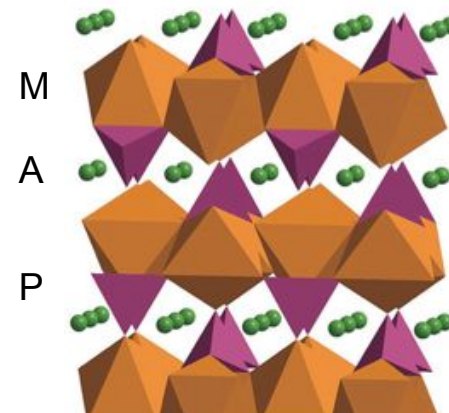
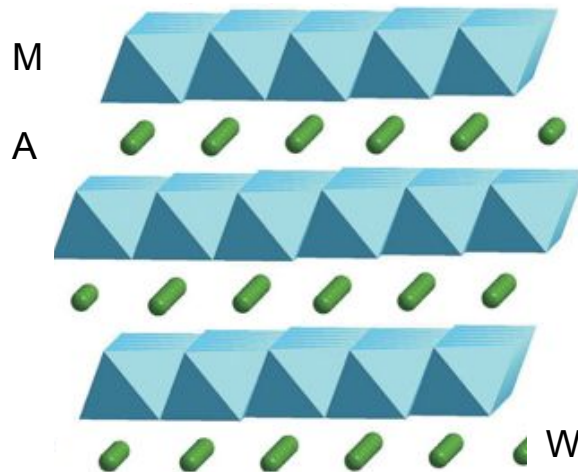
By segment Q1 2019–Q1 2024



How the metal-ion battery works



Cathode materials



Why TM metals are used ?

What is common between all cathode materials ?

Layered oxides AMO_2

A = Li, Na

M = Co, Mn, Ni

LiCoO_2

High capacity and voltage

Olivine-like AMPO_4

A = Li, Na

M = Fe, Mn, Co

LiFePO_4

High stability

Polyanion materials,

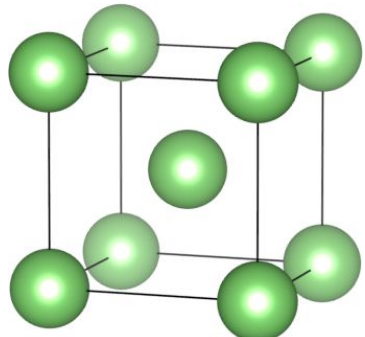
e.g. KVPO_4F ,

$\text{Na}_2\text{FePO}_4\text{F}$, etc.

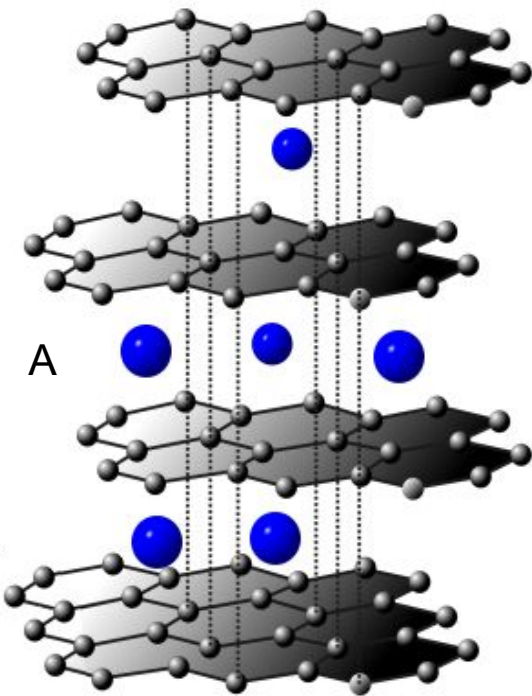
SO_4 , SiO_4 , BO_3

High rate, voltage, and stability

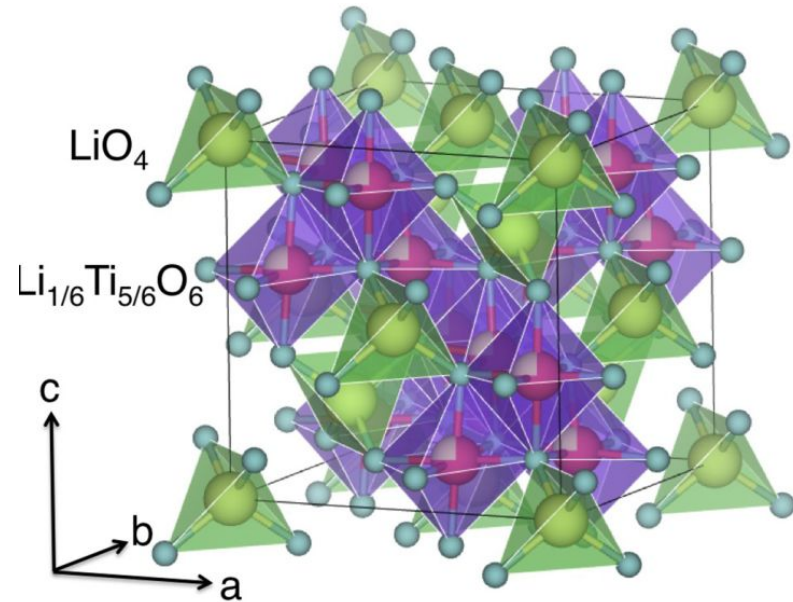
Anode materials



Metallic, Li, Na, K
Highest capacity
Highest energy

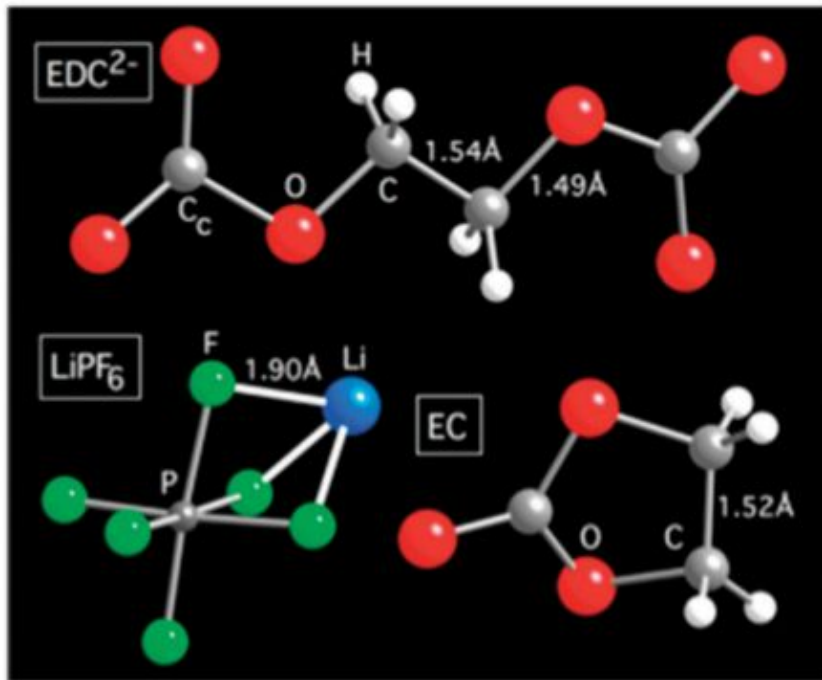


Graphite, A = Li, K
High capacity
High energy

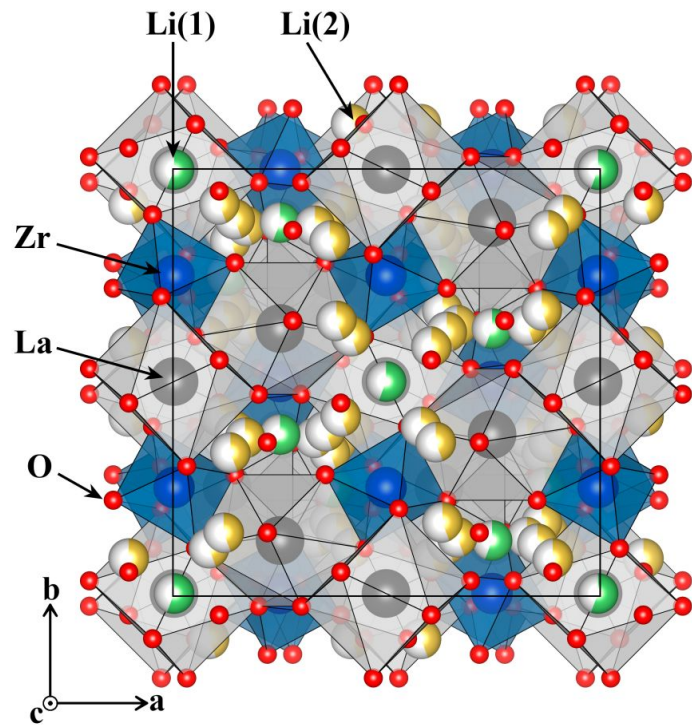


Titanate, spinel $\text{Li}_4\text{Ti}_5\text{O}_{12}$
High stability - >5000 of cycles
High charge rate (<30 minutes)

Electrolytes: liquid and solid



Li salts, such as LiPF_6 , are dissolved in organic solvents such as ethylene carbonate (EC), propylene carbonate (PC), dimethyl carbonate (DMC)



Solid electrolytes: $\text{Li}_{2.9}\text{PO}_{2.9}\text{N}_{0.5}$ (LIPON), $\text{Li}_6\text{PS}_5\text{X}$ (Argyrodite), $\text{Li}_7\text{La}_3\text{Zr}_2\text{O}_{12}$ (garnet)
More safe, problems with interface

How do the characteristics of a Li-ion battery are connected with the properties of energy materials?

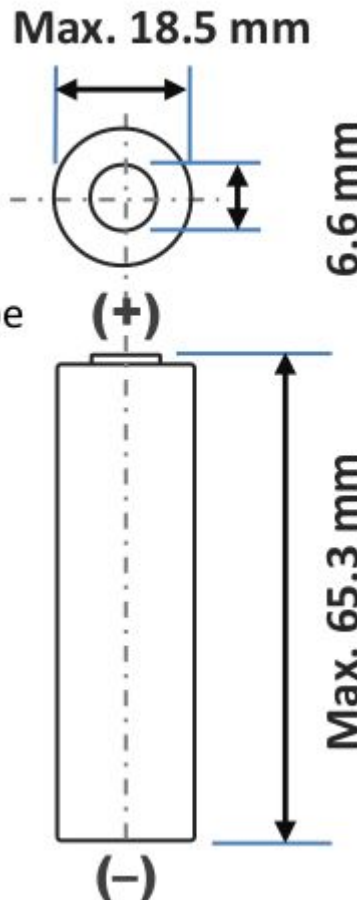
What properties of energy materials can be predicted with computer modeling?

Lithium Ion NCR18650F

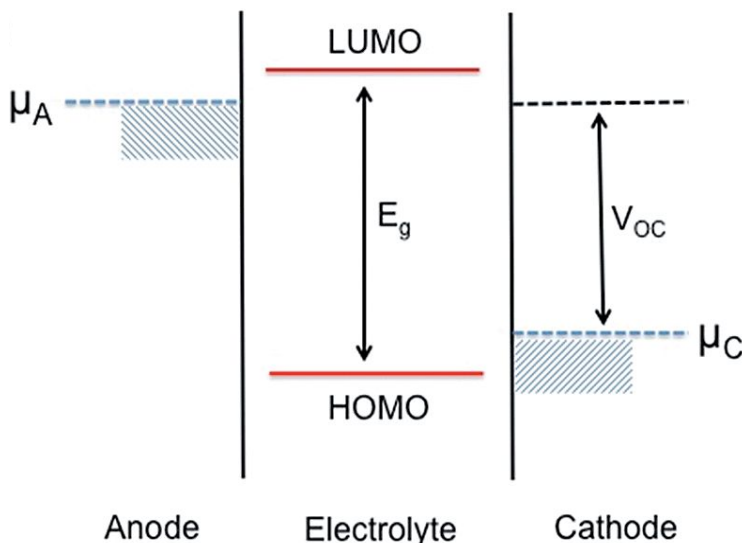
Specifications

Rated capacity ⁽¹⁾	Min. 2700mAh
Capacity ⁽²⁾	Min. 2750mAh Typ. 2900mAh
Nominal voltage	3.6V
Charging	CC-CV, Std. 1375mA, 4.20V, 4.0 hrs
Weight (max.)	46.5 g
Temperature	Charge*: 0 to +45°C Discharge: -20 to +60°C Storage: -20 to +50°C
Energy density ⁽³⁾	Volumetric: 577 Wh/l Gravimetric: 214 Wh/kg

Dimensions



Average intercalation voltage



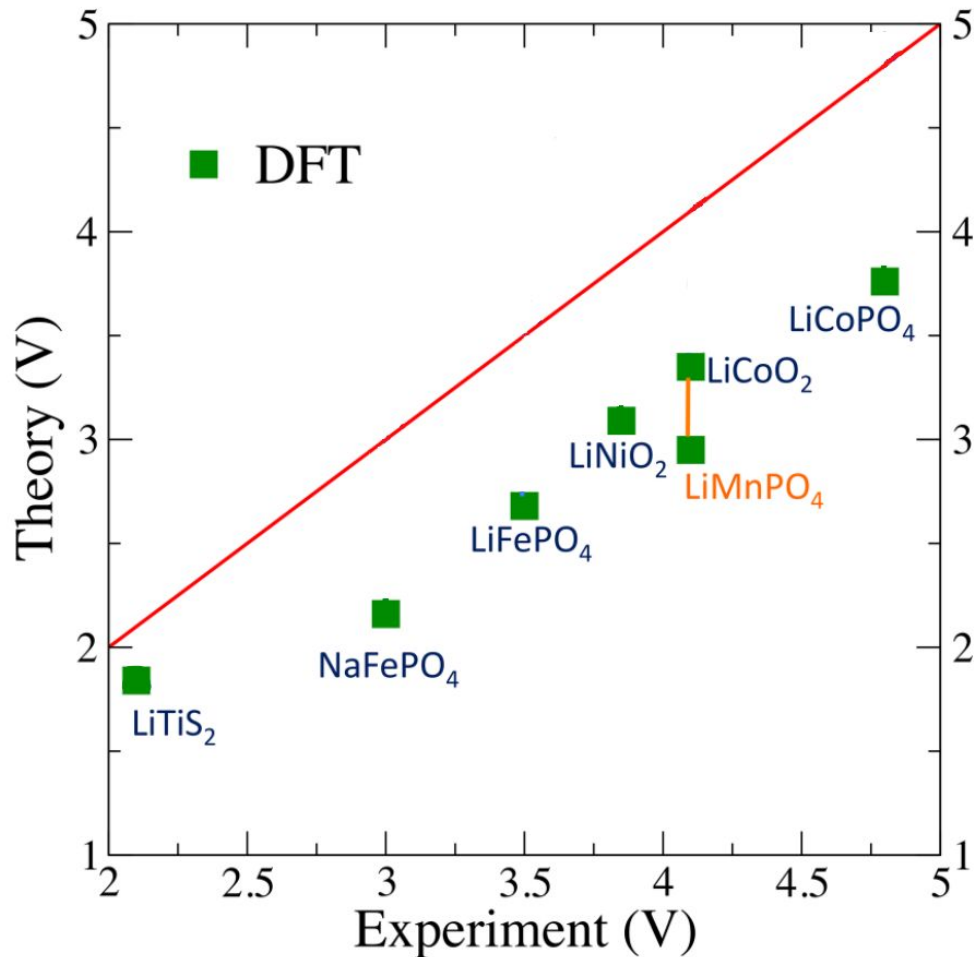
$$V = -\frac{\mu_A^C - \mu_A^A}{ze}$$

Li chemical potentials in
cathode and anode materials
transferred charge

- $\mu_u = H - TS$
- entropic contribution is small
- $H = E + PV$
- To a high accuracy V can be calculated from total energies at 0 K:

$$\bar{V}(x_1, x_2) \approx -\frac{E(\text{Li}_{x_1} \text{MO}_2) - E(\text{Li}_{x_2} \text{MO}_2) - (x_1 - x_2) E(\text{Li})}{(x_1 - x_2) F}$$

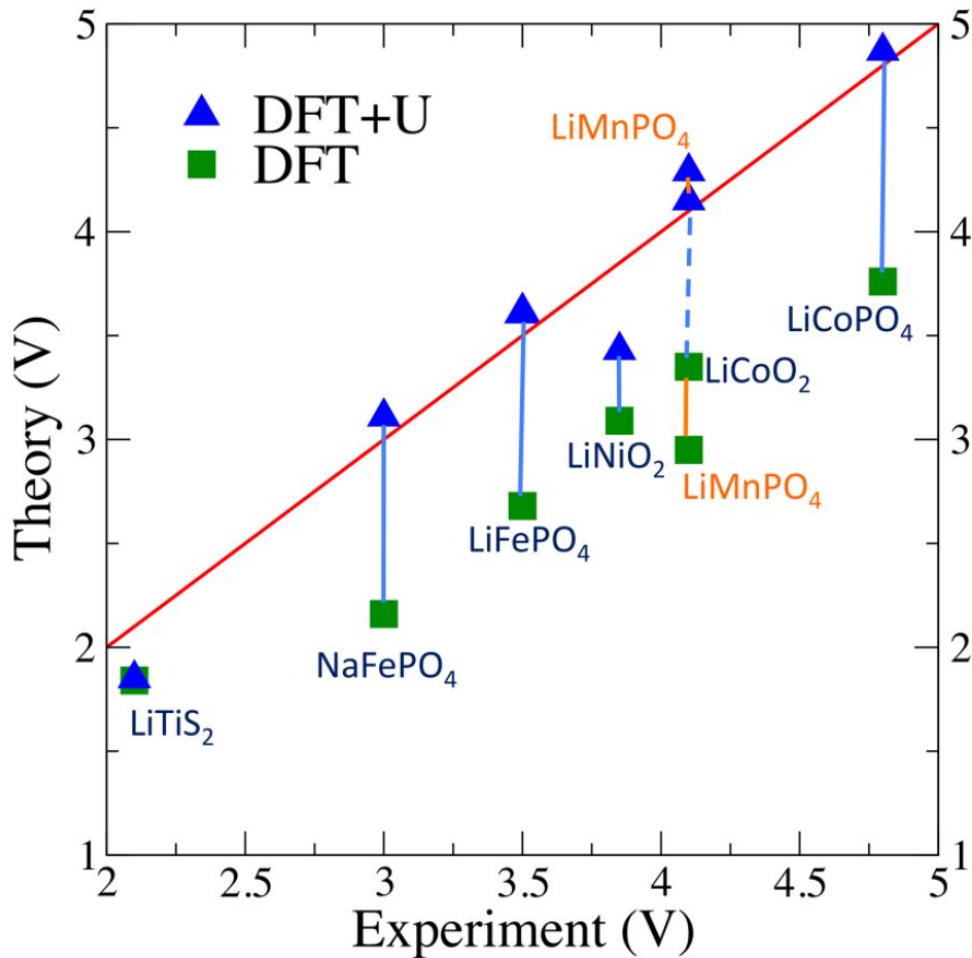
DFT underestimates voltage by ~1 V



How to correct?

Intercalation voltage predicted by DFT+U

- U is onsite repulsion added on d-orbitals of transition metals
- Allows to overcome the problem of electron delocalization in DFT
- Computational cheap
- Almost all other properties of metal oxides improved with DFT+U



DFT+U

$$E^{\text{DFT}+U}[n(\mathbf{r})] = E^{\text{DFT}}[n(\mathbf{r})] + E^{\text{Hub}}[n^{I\sigma}] - E^{\text{DC}}[N^{I\sigma}]. \quad (1)$$

$$E^U[n^{I\sigma}] = \sum_{I,\sigma} \frac{U^I}{2} \text{Tr}[n^{I\sigma}(1 - n^{I\sigma})]. \quad (2)$$

$$n_{mm'}^{I\sigma} = \sum_{\mathbf{k},v} f_{\mathbf{k},v}^\sigma \langle \psi_{\mathbf{k},v}^\sigma | P_{mm'}^I | \psi_{\mathbf{k},v}^\sigma \rangle, \quad (3)$$

$$P_{mm'}^I = |\phi_m^I\rangle\langle\phi_{m'}^I|, \quad (4)$$

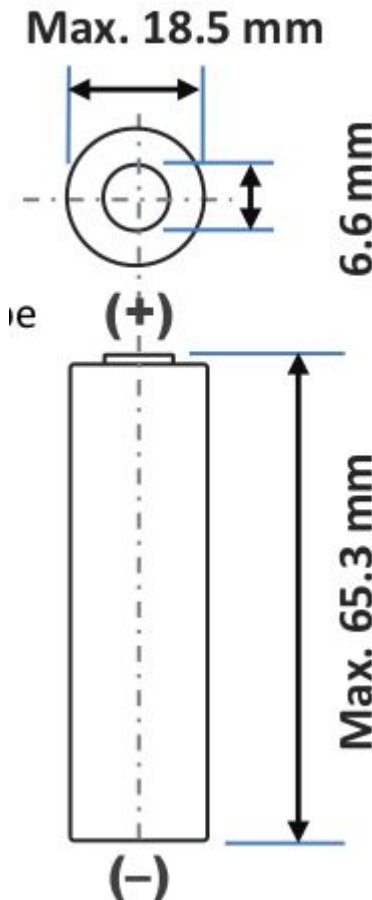
are d orbitals, localized on atom I

Lithium Ion NCR18650F

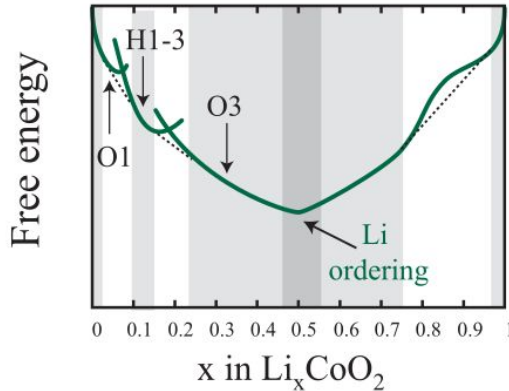
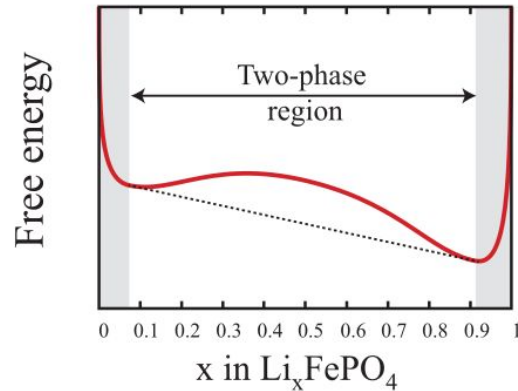
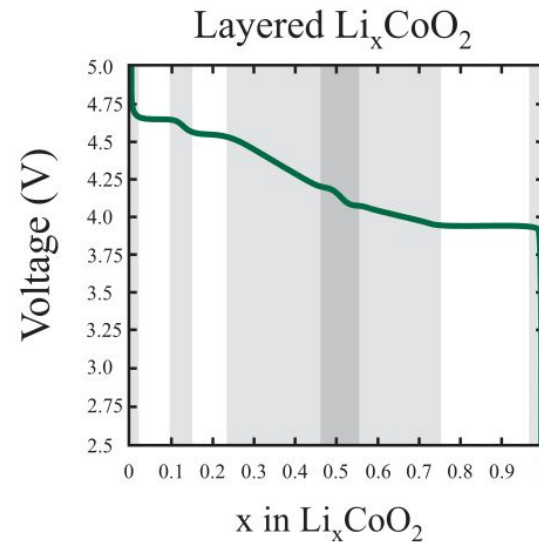
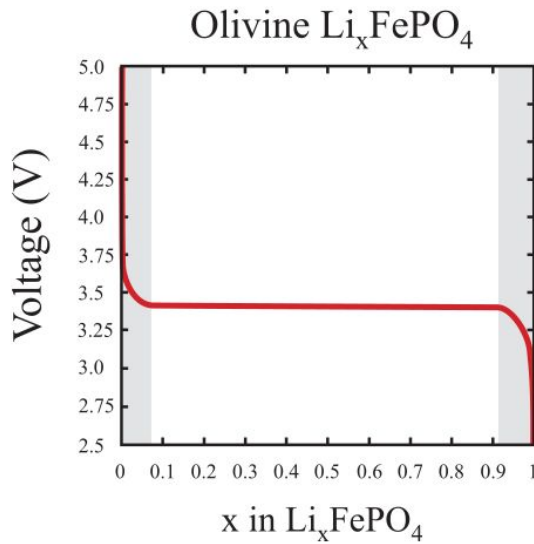
Specifications

Rated capacity ⁽¹⁾	Min. 2700mAh
Capacity ⁽²⁾	Min. 2750mAh Typ. 2900mAh
Nominal voltage	3.6V
Charging	CC-CV, Std. 1375mA, 4.20V, 4.0 hrs
Weight (max.)	46.5 g
Temperature	Charge*: 0 to +45°C Discharge: -20 to +60°C Storage: -20 to +50°C
Energy density ⁽³⁾	Volumetric: 577 Wh/l Gravimetric: 214 Wh/kg

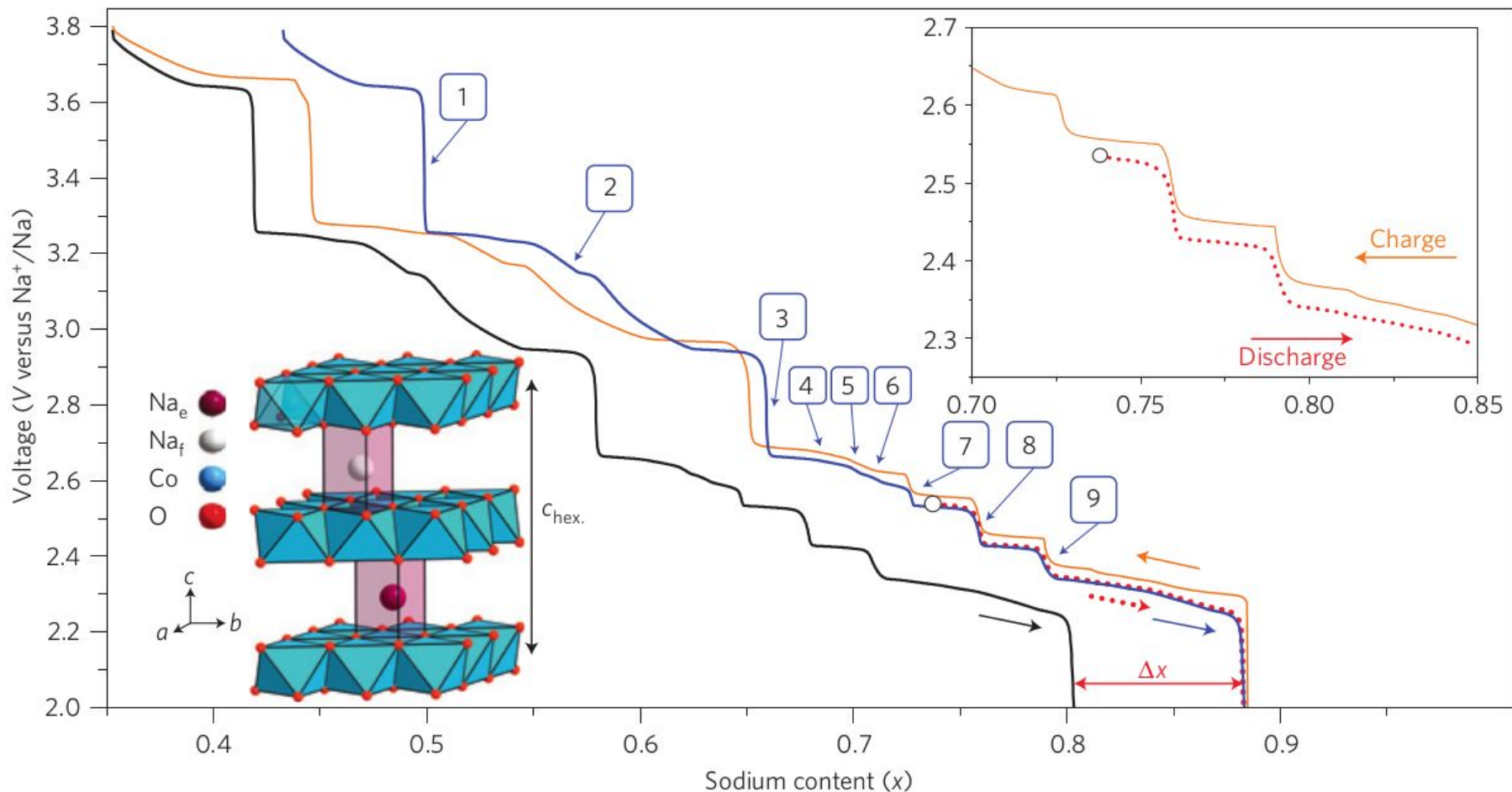
Dimensions



Voltage profiles



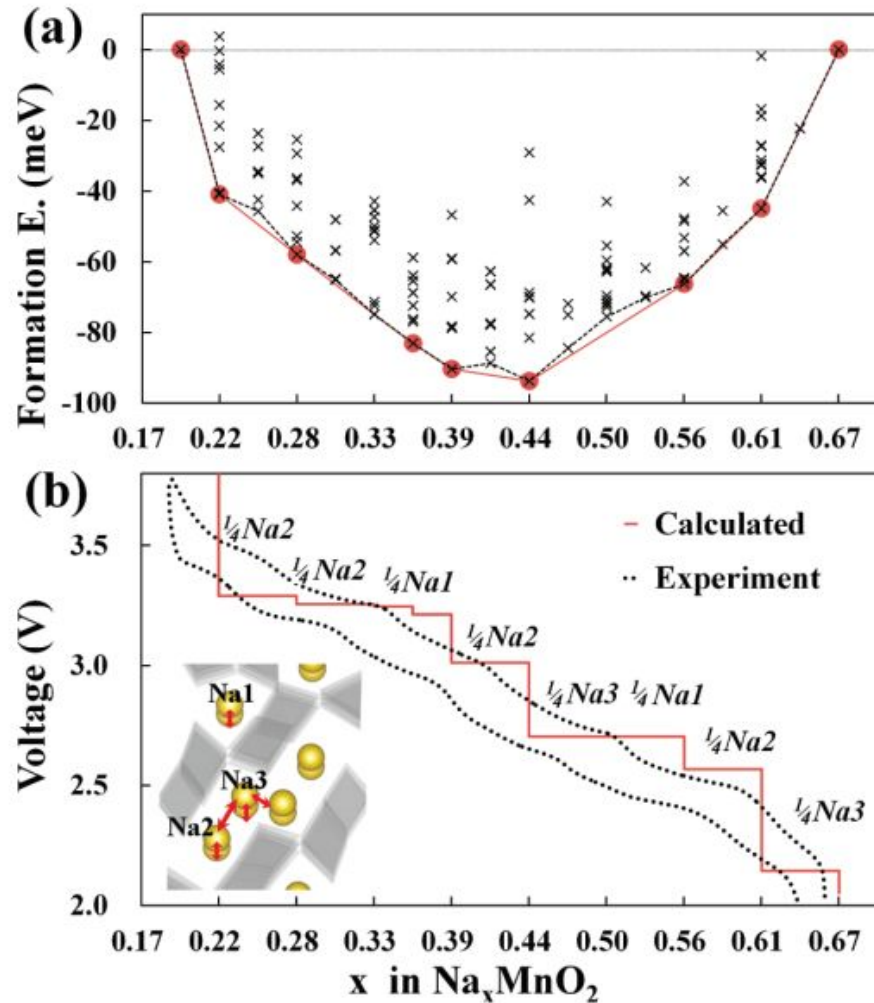
Voltage profile in NaCoO_2



Berthelot2011

Calculation of voltage profile $\text{Na}_{0.44}\text{MnO}_2$

$$E_f(\text{Li}_x\text{MO}_2) = E(\text{Li}_x\text{MO}_2) - x E(\text{LiMO}_2) - (1-x) E(\text{MO}_2),$$



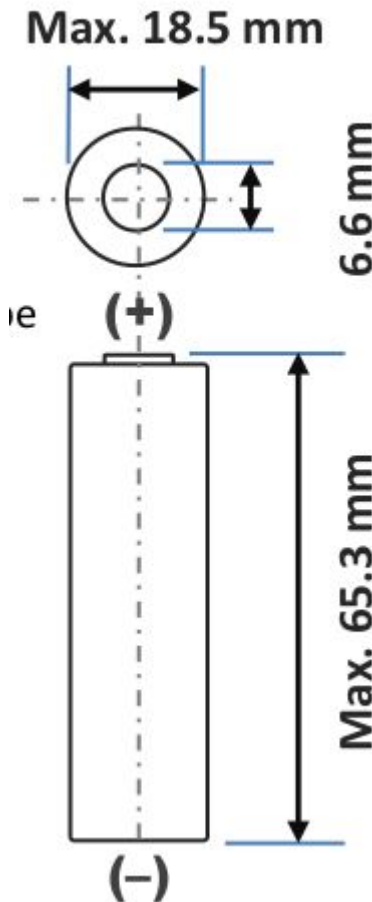
What about phase transitions due to temperature?

Lithium Ion NCR18650F

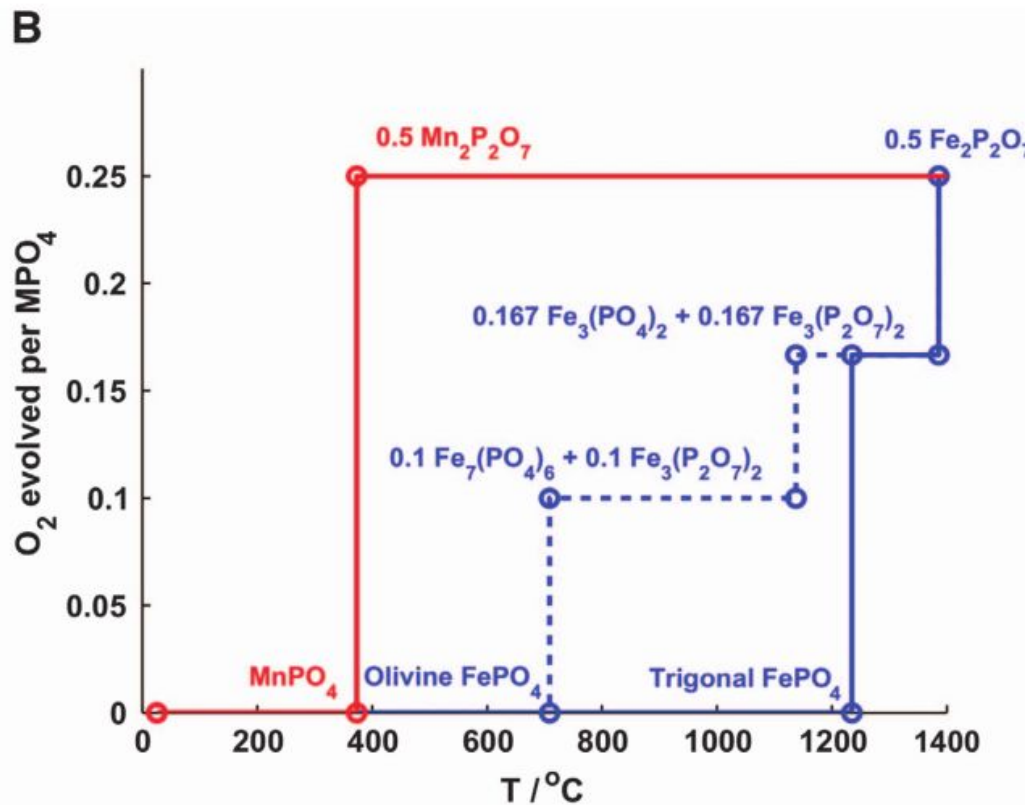
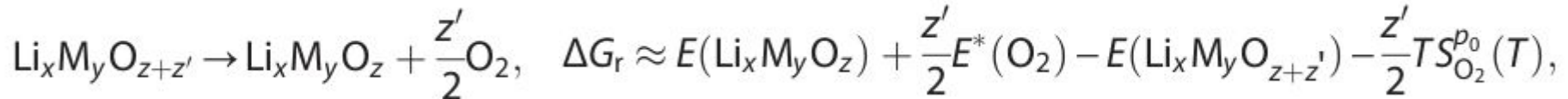
Specifications

Rated capacity ⁽¹⁾	Min. 2700mAh
Capacity ⁽²⁾	Min. 2750mAh Typ. 2900mAh
Nominal voltage	3.6V
Charging	CC-CV, Std. 1375mA, 4.20V, 4.0 hrs
Weight (max.)	46.5 g
Temperature	Charge*: 0 to +45°C Discharge: -20 to +60°C Storage: -20 to +50°C
Energy density ⁽³⁾	Volumetric: 577 Wh/l Gravimetric: 214 Wh/kg

Dimensions



Thermal stability of cathodes



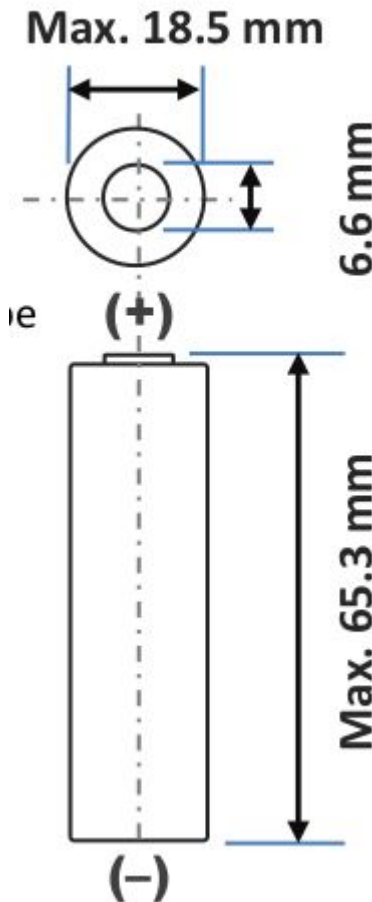
Urban, A. et al.// *npj Computational Materials* 2.1 (2016): 1-13.

Lithium Ion NCR18650F

Specifications

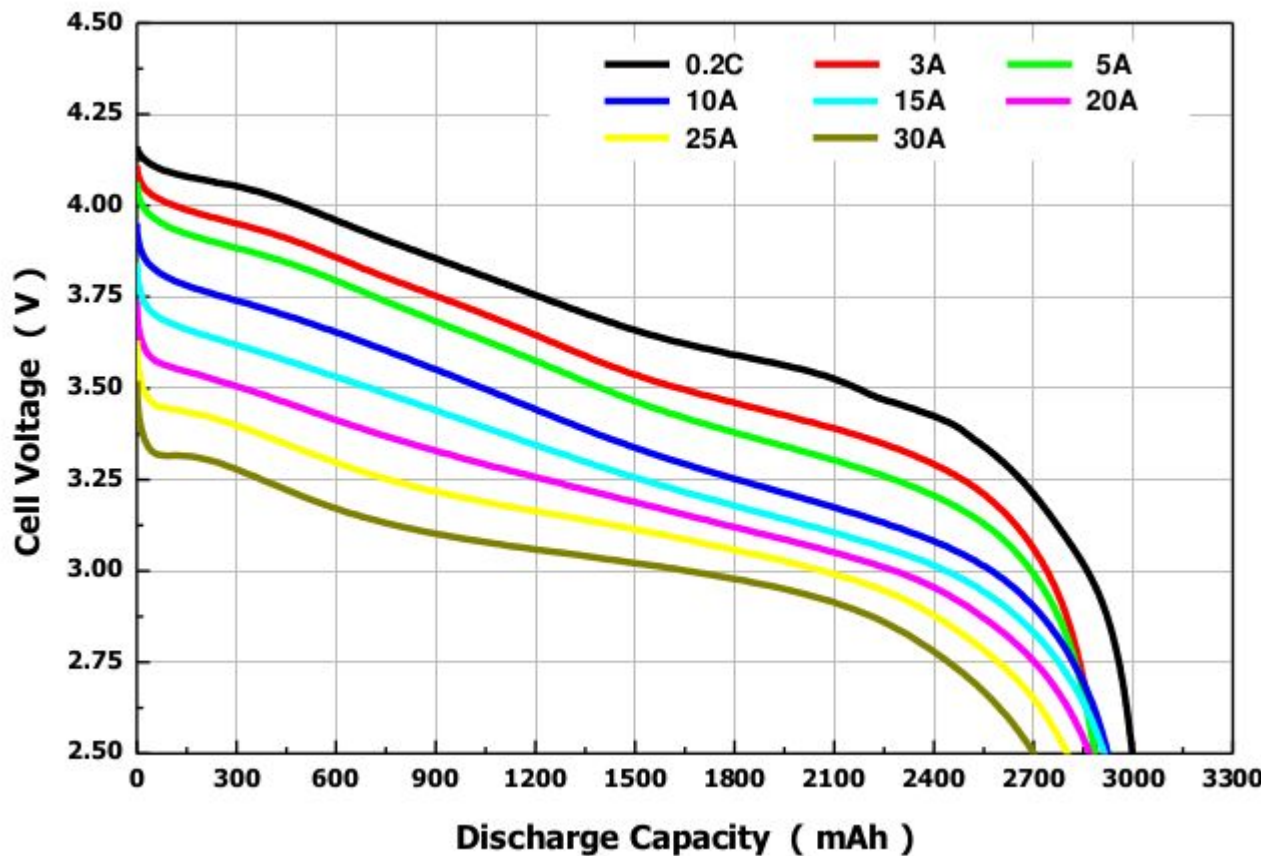
Rated capacity ⁽¹⁾	Min. 2700mAh
Capacity ⁽²⁾	Min. 2750mAh Typ. 2900mAh
Nominal voltage	3.6V
Charging	CC-CV, Std. 1375mA, 4.20V, 4.0 hrs
Weight (max.)	46.5 g
Temperature	Charge*: 0 to +45°C Discharge: -20 to +60°C Storage: -20 to +50°C
Energy density ⁽³⁾	Volumetric: 577 Wh/l Gravimetric: 214 Wh/kg

Dimensions



Galvanostatic curves at different C-rates

- 1C current charge/discharge battery in one hour



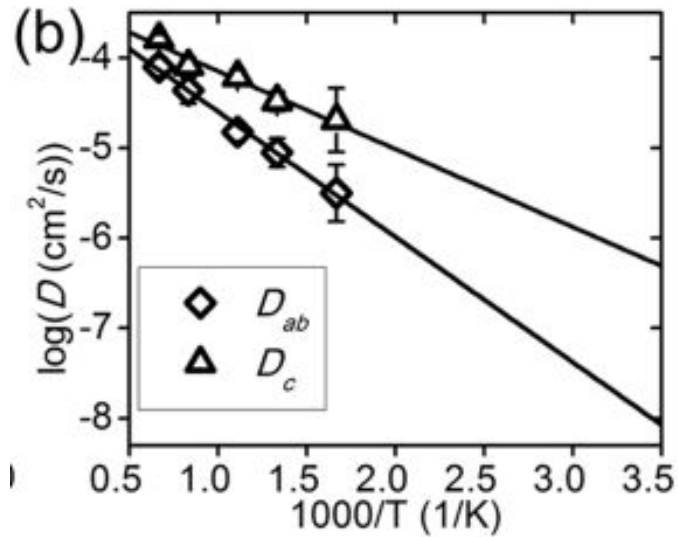
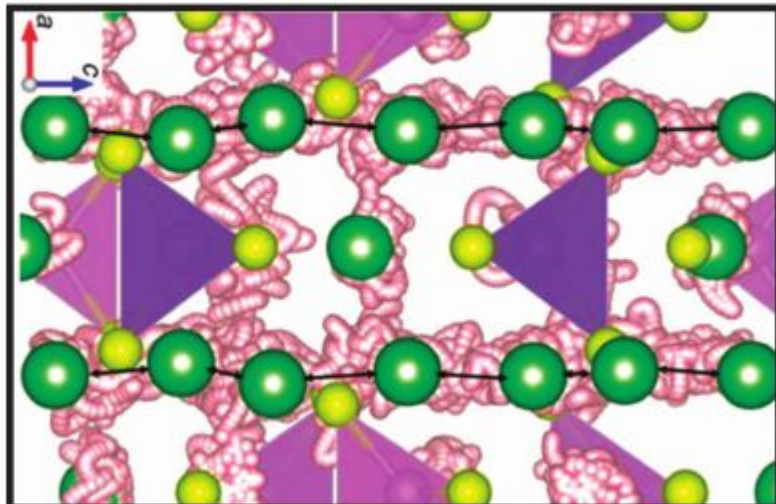
- At higher currents voltage drops by IR, where R depends on **ionic conductivity of electrode materials** and electrolyte, and charge-transfer resistance

Ionic conductivity, Ab initio MD

$$\sigma(T) = \frac{N_{\text{Li}}}{V} \frac{e^2}{k_B T} D(T),$$

Nernst–Einstein relation for ionic conductivity. N_{Li} is the number of lithium ions, V is the volume of the simulation cell

Li trajectories in $\text{Li}_{10}\text{GeP}_2\text{S}_{12}$ at 900 K



$$D(T) \approx D_0 e^{-\frac{E_a}{k_B T}},$$

Arrhenius law: E_a is activation energy for diffusion

Urban, A. et al.// *npj Computational Materials* 2.1 (2016): 1-13.

Mo, Yifei, Shyue Ping Ong, and Gerbrand Ceder. "Chemistry of Materials" 24.1 (2012): 15-17.

Diffusivity based on 0 K migration barriers

Rate of the hopping process

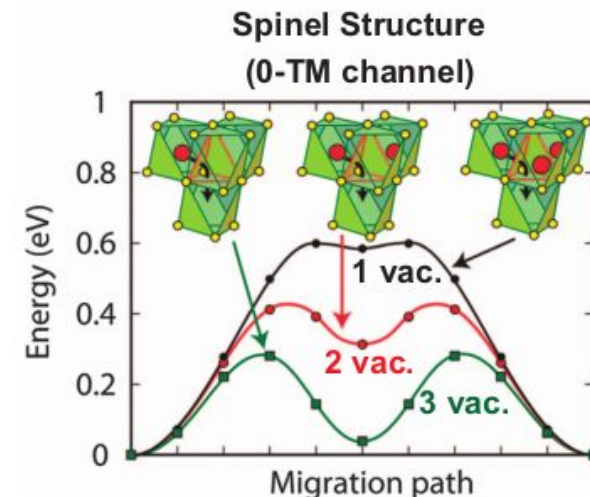
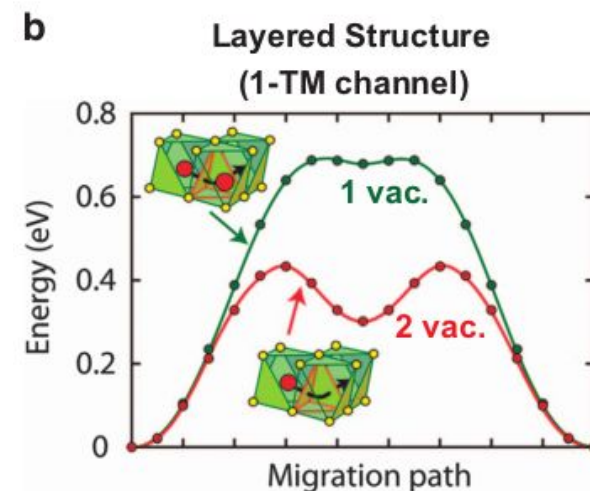
$$k(T) = \nu^*(T) e^{-\frac{\Delta G^\ddagger(T)}{k_B T}},$$

ν^* is temperature-dependent effective attempt frequency, ΔG^\ddagger is Gibbs free energy of activation (migration barrier)

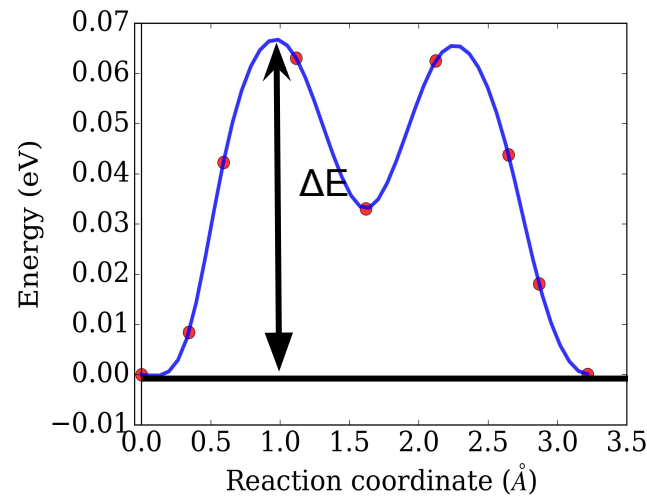
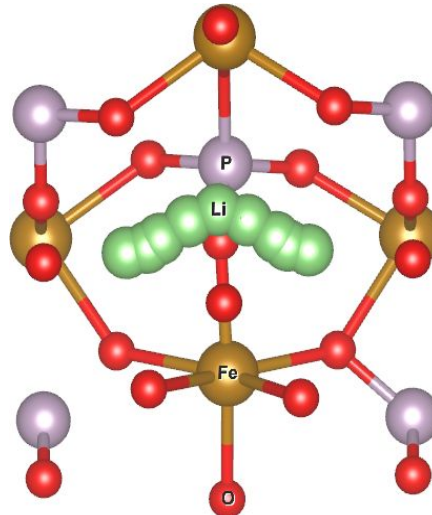
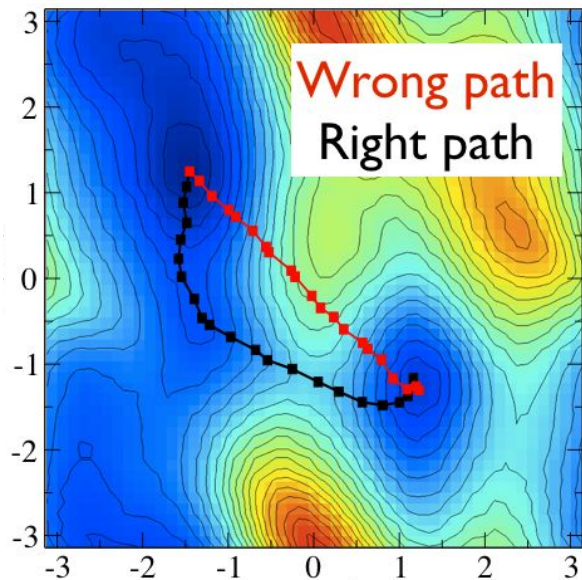
$$D \approx g \cdot a^2 \cdot k,$$

a is hopping distance, g is geometrical factor (~ 1)

Typical values for the prefactor ν^* are 10^{11} to 10^{13} s^{-1}



NEB method for finding saddle points



Nudged elastic band method (NEB) is used to find minimum energy paths and migration barriers at saddle points.

The spring forces keep the images spaces equally, allowing to propagate a chain towards minimum energy path.

Modeling of liquid electrolyte

Solvent	Structure	M. Wt	T _m /°C	T _b /°C	η/cP 25 °C	ϵ 25 °C
EC		88	36.4	248	1.90 (40 °C)	89.78
PC		102	-48.8	242	2.53	64.92
Li Salts						

Marcinek, M., et al. *Solid State Ionics* 276 (2015): 107-126.

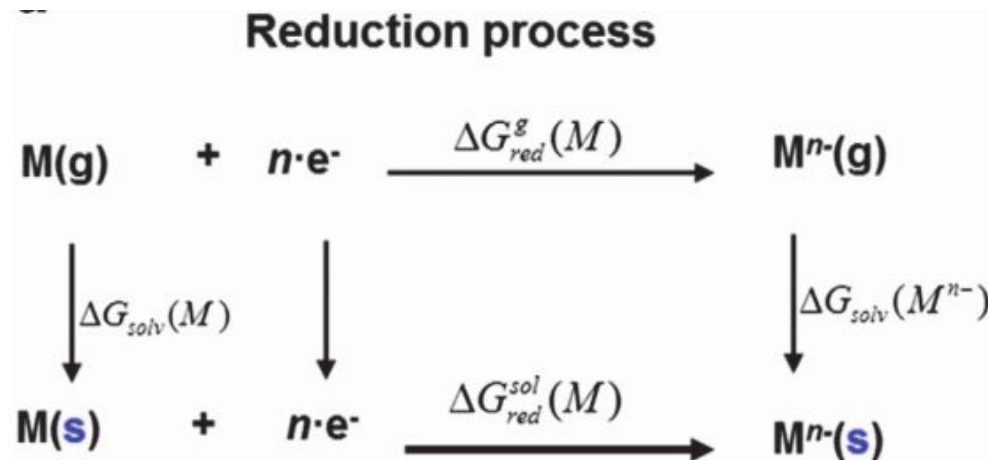
D. Aksyonov, Skoltech, AMM

Bogle, X, et al. *The journal of physical chemistry letters* 4.10 (2013): 1664-1668.

29/72

Electrochemical stability of electrolytes

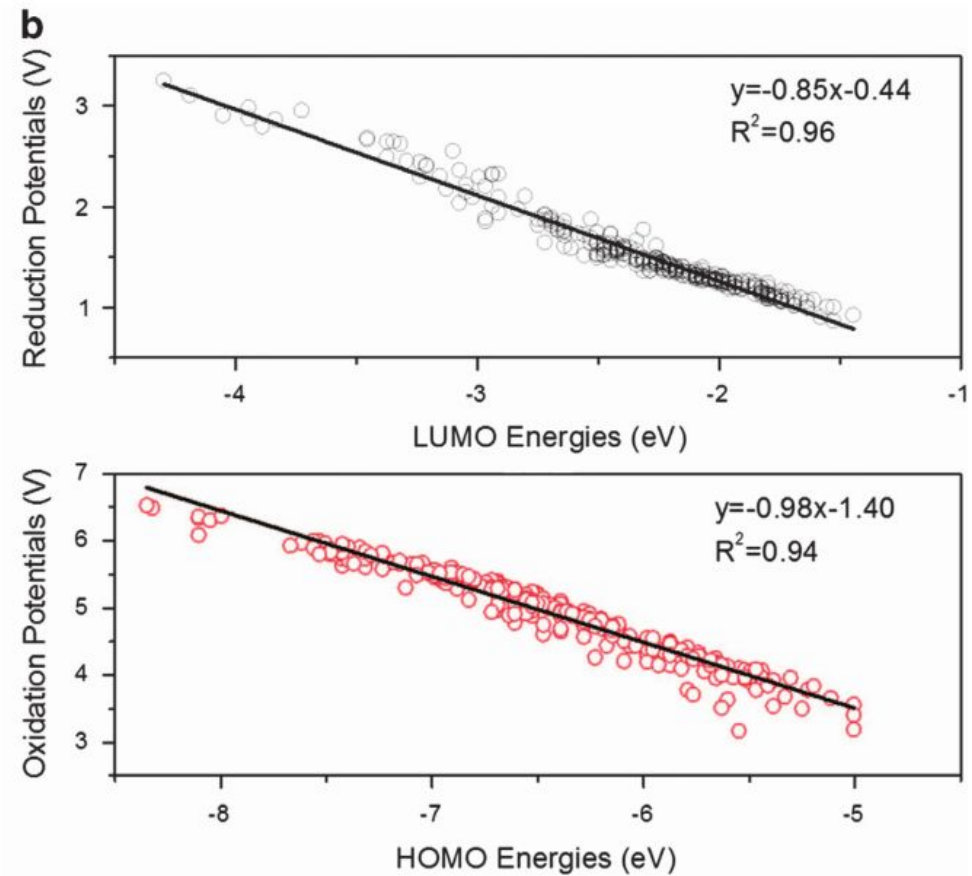
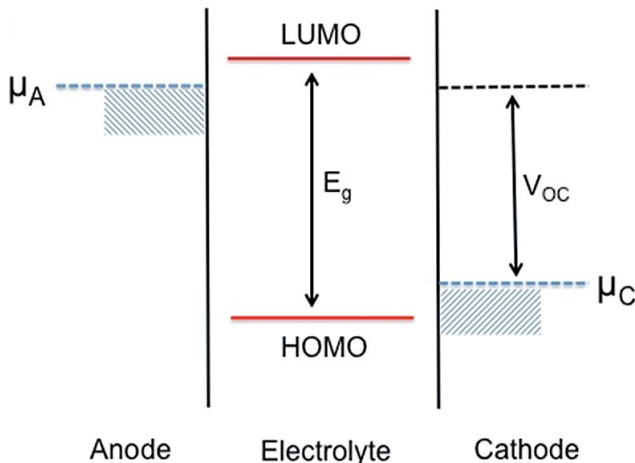
reduction : $\Delta G_{\text{red}}^{\text{s}} = G[\text{M}^{n-}(\text{s})] - G[\text{M}(\text{s})] - nG[\text{e}^-(\text{s})]$
oxidation : $\Delta G_{\text{ox}}^{\text{s}} = G[\text{M}^{n+}(\text{s})] + nG[\text{e}^-(\text{s})] - G[\text{M}(\text{s})],$



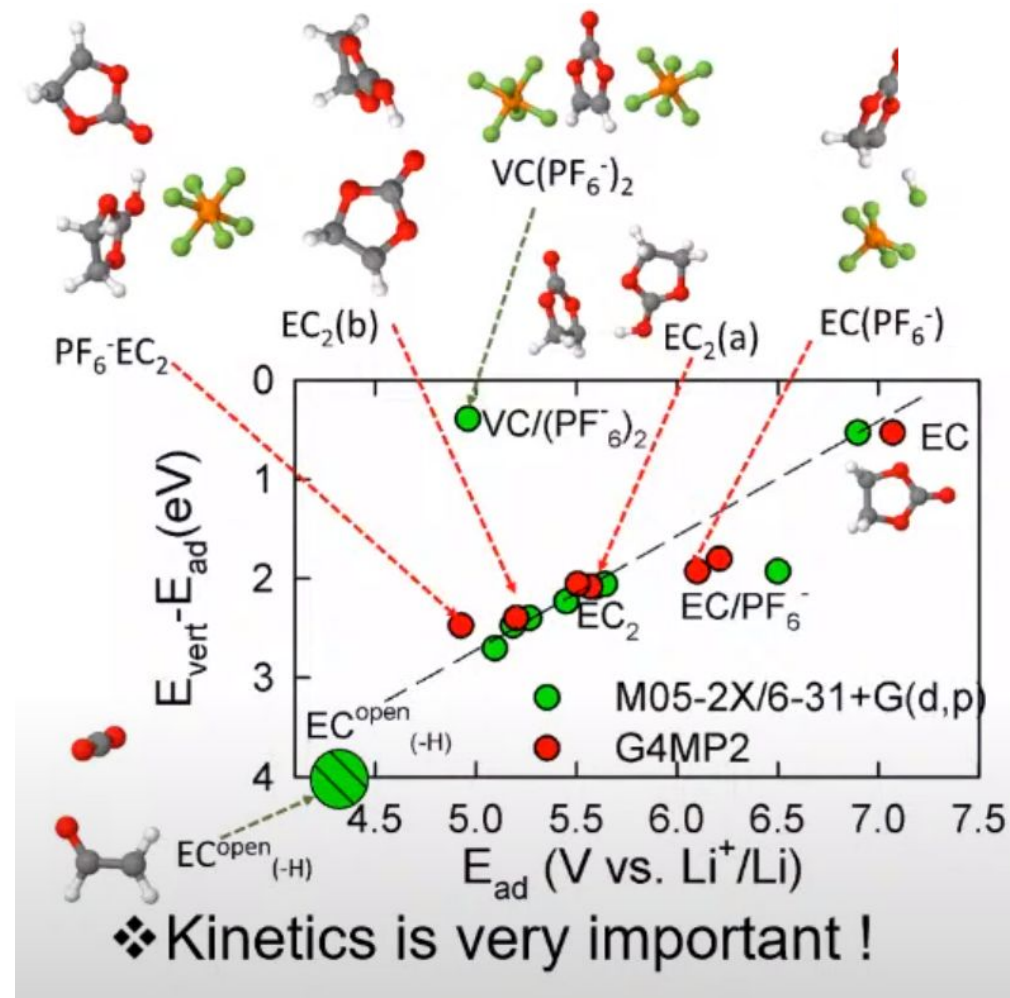
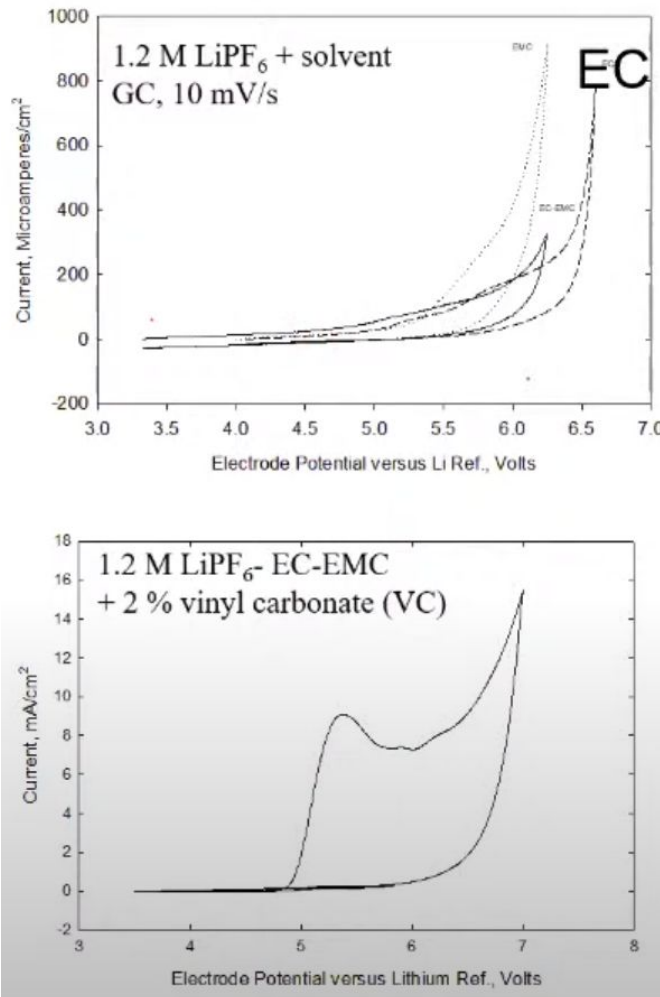
$$\Delta G_{\text{red}}^{\text{sol}}(M) = \Delta G_{\text{red}}^{\text{g}}(M) + \Delta G_{\text{sol}}(M^{n-}) - \Delta G_{\text{sol}}(M)$$

X. Zhang, *Journal of The Electrochemical Society* 148.5 (2001): E183-E188.

HOMO and LUMO for electrolytes screening



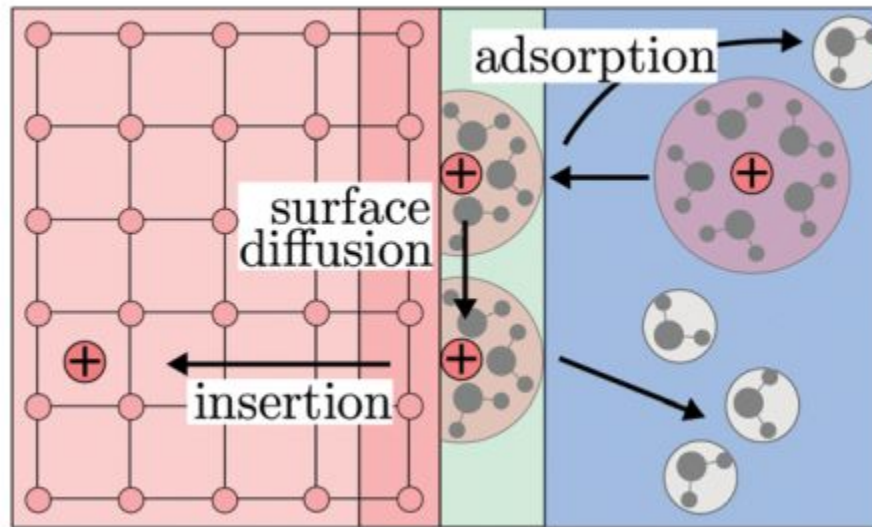
Prediction of EC and VC oxidation



O. Borodin, *Nanotechnology* 26 (2015) 354003

Electrolyte/electrode interface the largest challenge for modelling now

Diffusion is only half of the story, kinetics of interphase charge transfer is highly important



Li, Yunsong, and Yue Qi. "Energy landscape of the charge transfer reaction at the complex Li/SEI/electrolyte interface." *Energy & Environmental Science* 12.4 (2019): 1286-1295.

Lück, Jessica, and Arnulf Latz. "Modeling of the electrochemical double layer and its impact on intercalation reactions." *Physical Chemistry Chemical Physics* 20.44 (2018): 27804-27821.

Methods for battery materials modeling

Cathodes, anodes, solid state conductors:

- Phase stability (DFT+U, Hybrid)
- Intercalation voltages and intercalation mechanism (DFT+U, Hybrid)
- Diffusivity of cations (DFT, MD)
- Defects and influence on properties(DFT+U)

Liquid electrolytes (DFT, MD):

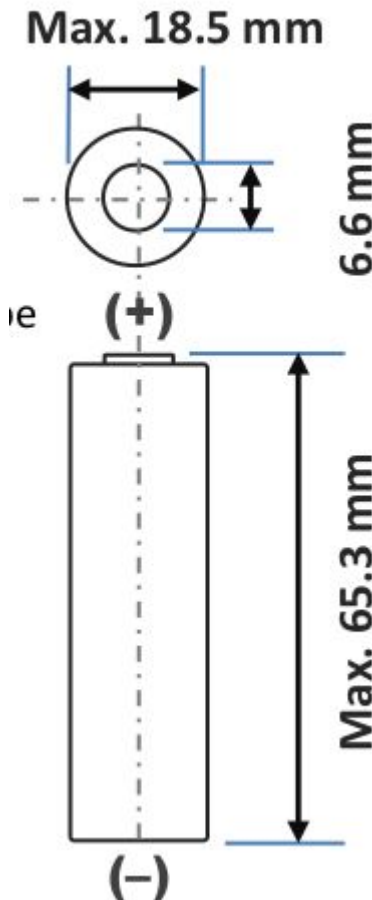
- Solvation energies (MP2, CI, CC, DFT)
- Electrolyte stability (MP2, CI, CC, DFT)

Lithium Ion NCR18650F

Specifications

Rated capacity ⁽¹⁾	Min. 2700mAh
Capacity ⁽²⁾	Min. 2750mAh Typ. 2900mAh
Nominal voltage	3.6V
Charging	CC-CV, Std. 1375mA, 4.20V, 4.0 hrs
Weight (max.)	46.5 g
Temperature	Charge*: 0 to +45°C Discharge: -20 to +60°C Storage: -20 to +50°C
Energy density ⁽³⁾	Volumetric: 577 Wh/l Gravimetric: 214 Wh/kg

Dimensions



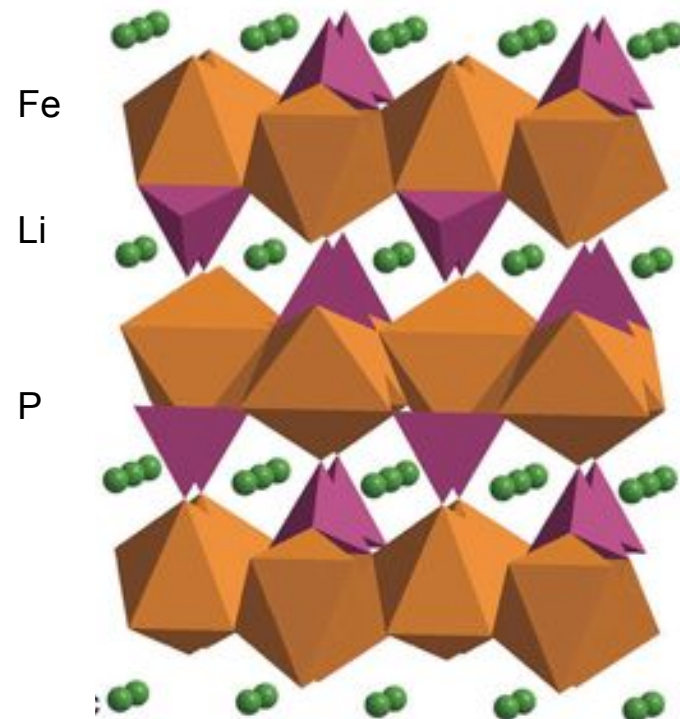
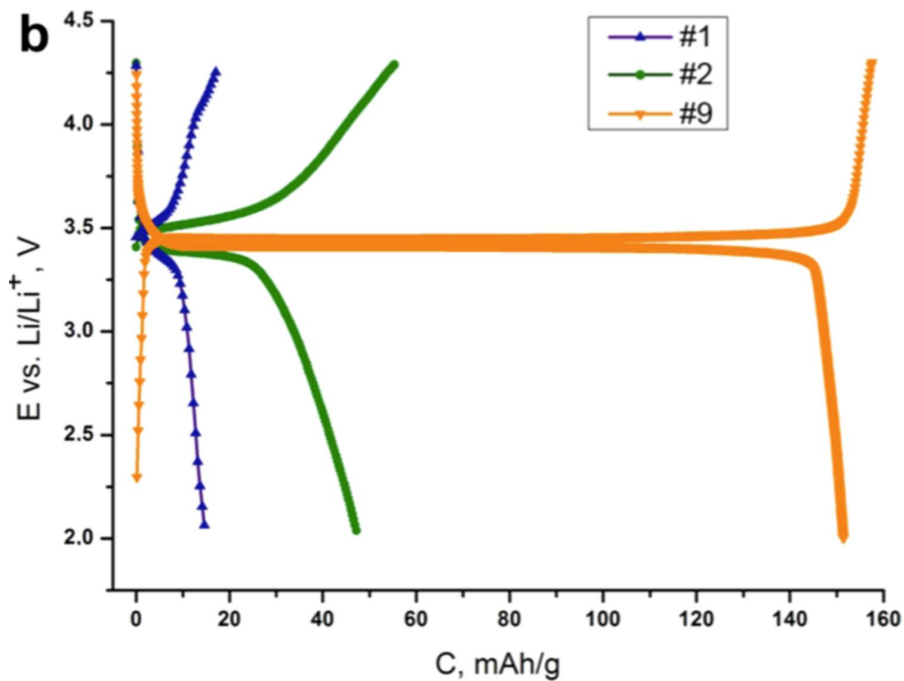
Capacity (mAh/g)

$$C_{\max} = \frac{nF}{3.6 \cdot MW}.$$

n - number of electrons inserted
MW - molecular weight
F is Faraday constant

- The formula gives you theoretical capacity per electrode. Due to **instability of material and defects**, the amount of Li that can be extracted is limited, therefore practical capacity is only 50-90% of theoretical
- Once both anode and cathode, electrolyte and case are taken into account the capacity is further decrease by 50-80%

LiFePO_4 developed in Skoltech and MSU



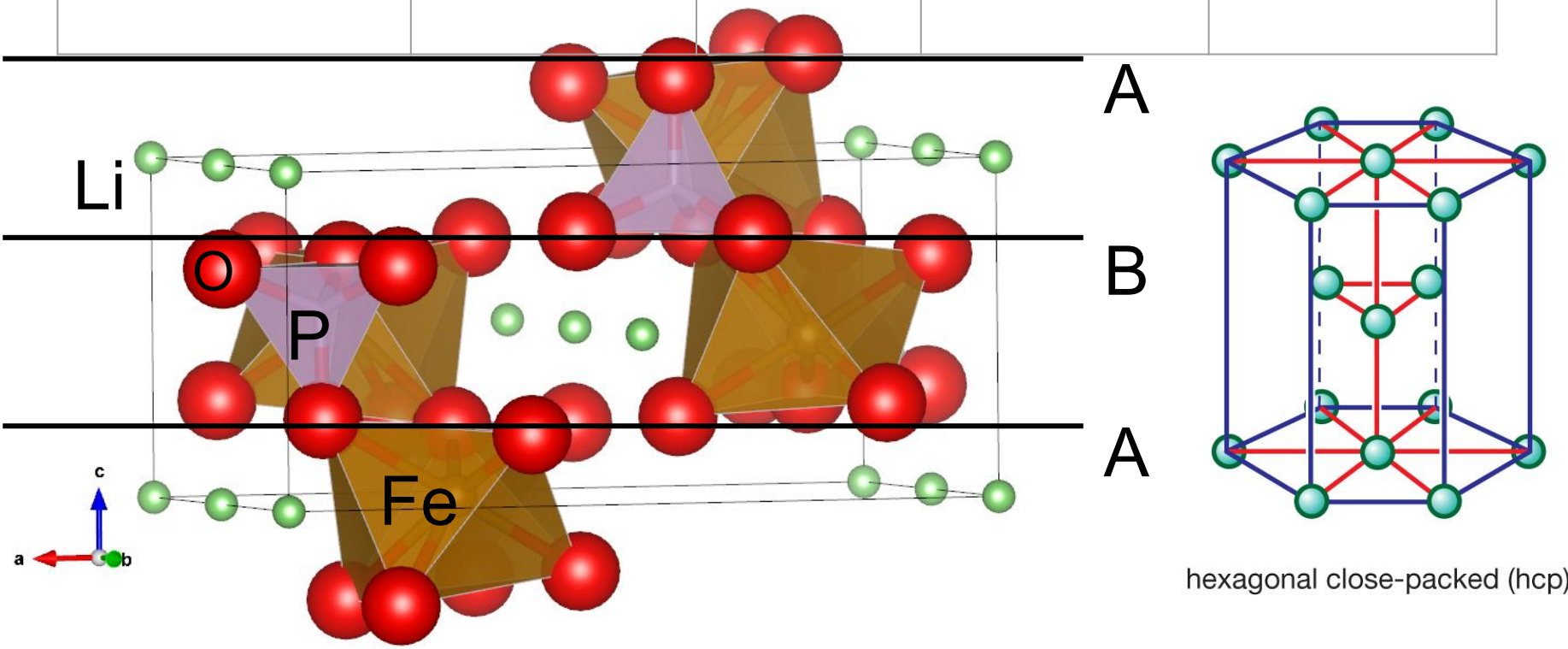
LiFePO_4 30% of market share in Li-ion industry

- First commercialized use of A123 battery in ~2005 in DeWalt power tools [1]
- Used mostly in electric buses and smart grids in China [2]
- Due to lower energy density of LFP (175 Wh/kg) autoproducers focused on layer oxides (250 Wh/kg)
- But the growth of electric cars market posed risks for Ni and Co price rise and Tesla started to use LFP batteries in mass-market cars
- The forecast: LFP is the only alternative for mass-produced energy storage

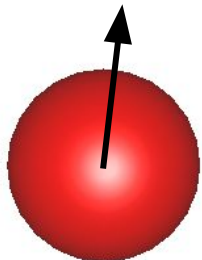


Crystal structure of LiFePO_4 (LFP)

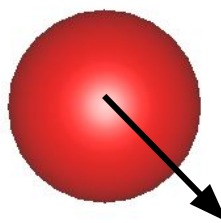
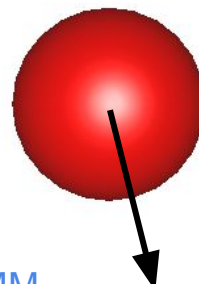
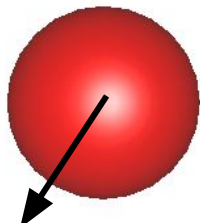
Formula	mineral	a, Å	b	c
LiFePO_4	triphylite	10.33	6.00	4.70



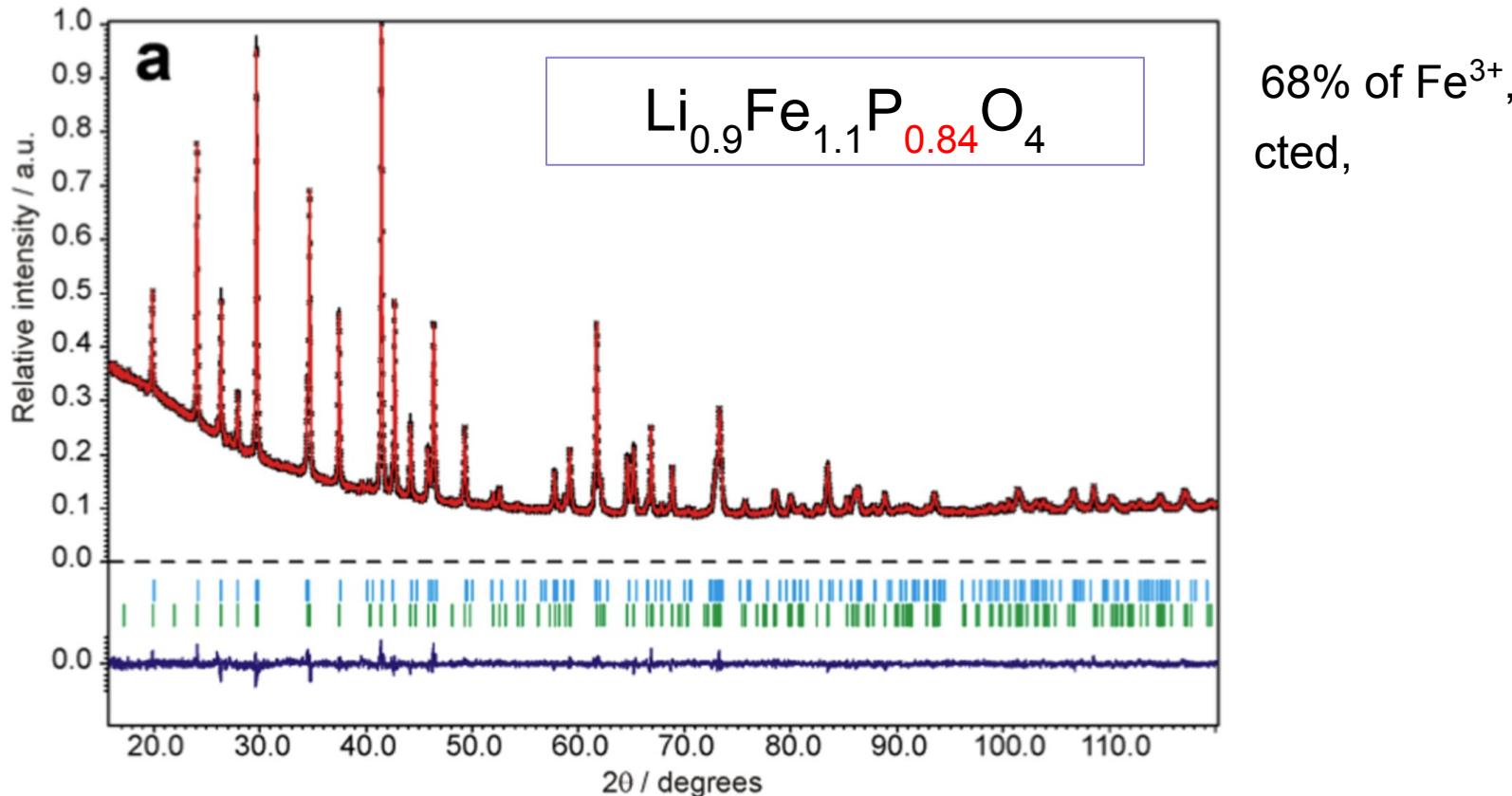
Point defects in LiFePO₄



↳ Bounced in LFP material and
needed defect-free?
↳ d vacancies in P sublattice
[7, 12, 4261–4273]



Defective LFP with P vacancies was confirmed in a joined study by Skoltech and MSU



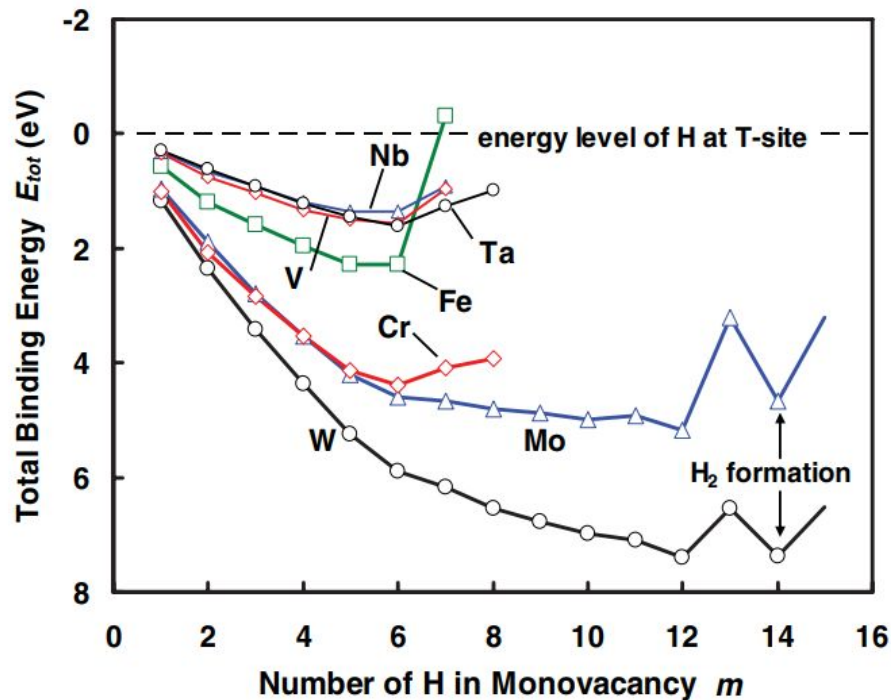
Sumanov, V D., D.A. Aksyonov, O.A. Drozhzhin, et al. // *Chemistry of Materials* 31, no. 14 (2019): 5035-5046.

How to explain P vacancies?

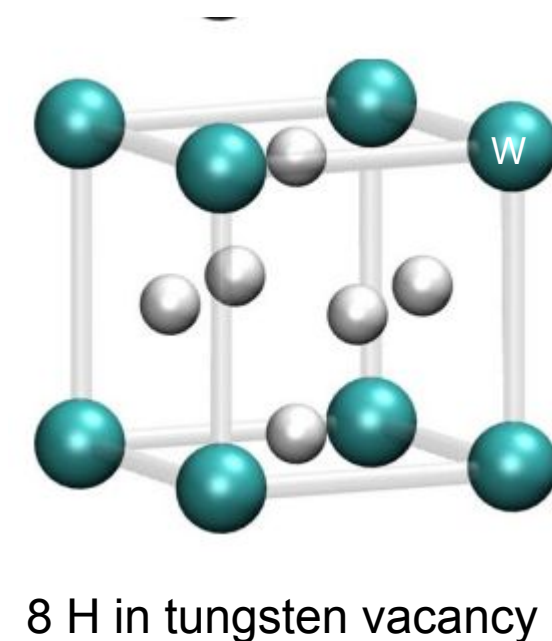
- incorporation of impurities, e.g. carbon,
- impurity phases
- inaccuracy in refinement, oxygen excess
- Hydrogen? quite possible taking into account that hydrothermal synthesis was used

Inspiration from metals

In metals, hydrogen is usually trapped in vacancies
E.g. up to 12 hydrogens fit inside tungsten vacancy



PHYSICAL REVIEW B 85, 094102 (2012)



PHYSICAL REVIEW B 82, 094102 2010

How could structural OH defects have been missed in LiFePO₄?



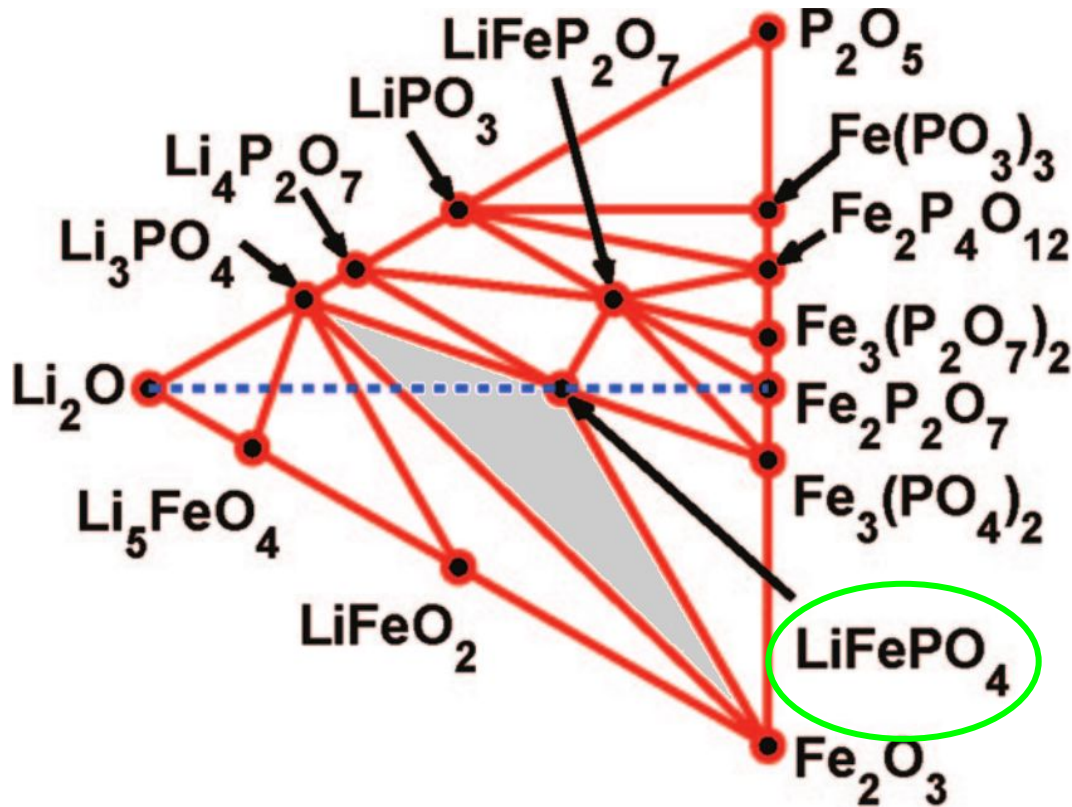
papers were published on LiFePO₄ material and et al. have proposed possibility of OH defects at Li are never confirmed.

“pharnet”-like OH defects are well known in the s n(Mg,Fe)₂SiO₄·mMg₂V_{Si}(OH)₄

calculated formation energies of OH defects using ods

Libowitzky, E., Beran, A., Wieczorek, A.K. et al. On the presence of a hydrous component in a gemstone variety of intermediate olivine-type triphylite-lithiophilite, Li(Fe,Mn)PO₄. *Miner Petrol* 105, 31–39 (2012).

Li-Fe-P-O phase diagram, $\mu(\text{O}_2) = -12.4 \text{ eV}$



Li_3PO_4 - LiFePO_4 - Fe_2O_3 region
is stable for $\mu(\text{O}_2)$ from
 -13.0 eV to -11.5 eV

$$\mu(\text{Fe}) = 1/2 [\mu(\text{Fe}_2\text{O}_3) - 3/2 \mu(\text{O}_2)]$$

$$\begin{aligned} \mu(\text{Li}) = 1/2 & [\mu(\text{Li}_3\text{PO}_4) - \mu(\text{LiFePO}_4) + \\ & + \mu(\text{Fe})] \end{aligned}$$

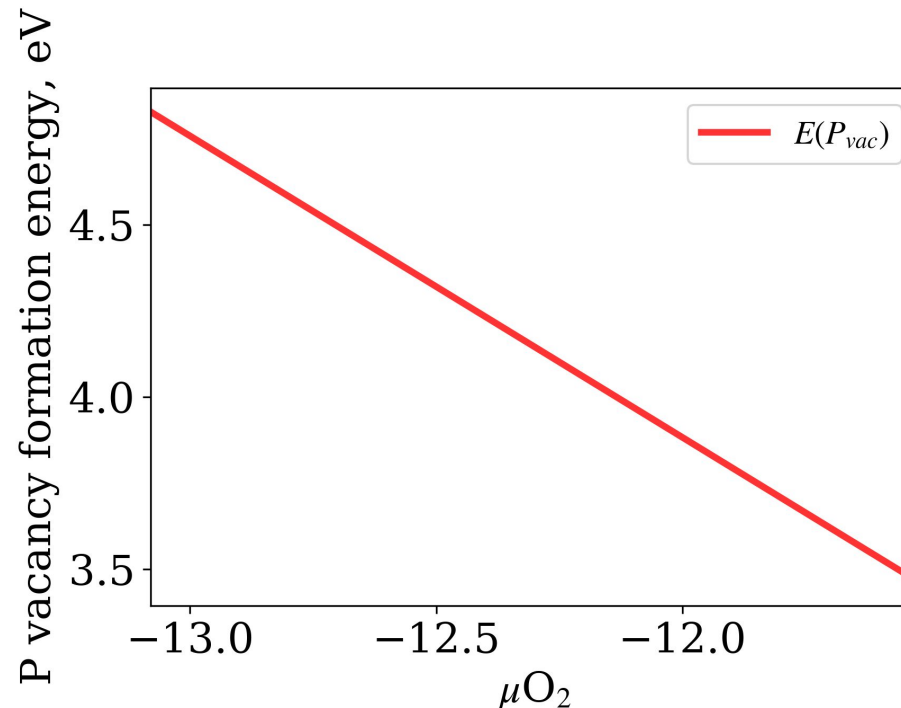
$$\begin{aligned} \mu(\text{P}) = 1/2 & [3 \mu(\text{LiFePO}_4) - \mu(\text{Li}_3\text{PO}_4) \\ & - 3 \mu(\text{Fe}) - 4 \mu(\text{O}_2)], \end{aligned}$$

$$\mu(\text{H}) = 1/2 [\mu(\text{H}_2\text{O}) - 1/2 \mu(\text{O}_2)]$$

- Ong, S.P., Wang, L., Kang, B. and Ceder, G. Li-Fe-P-O₂ Phase Diagram from First Principles Calculations. Chemistry of Materials. 20, 5 (Mar. 2008), 1798–1807.

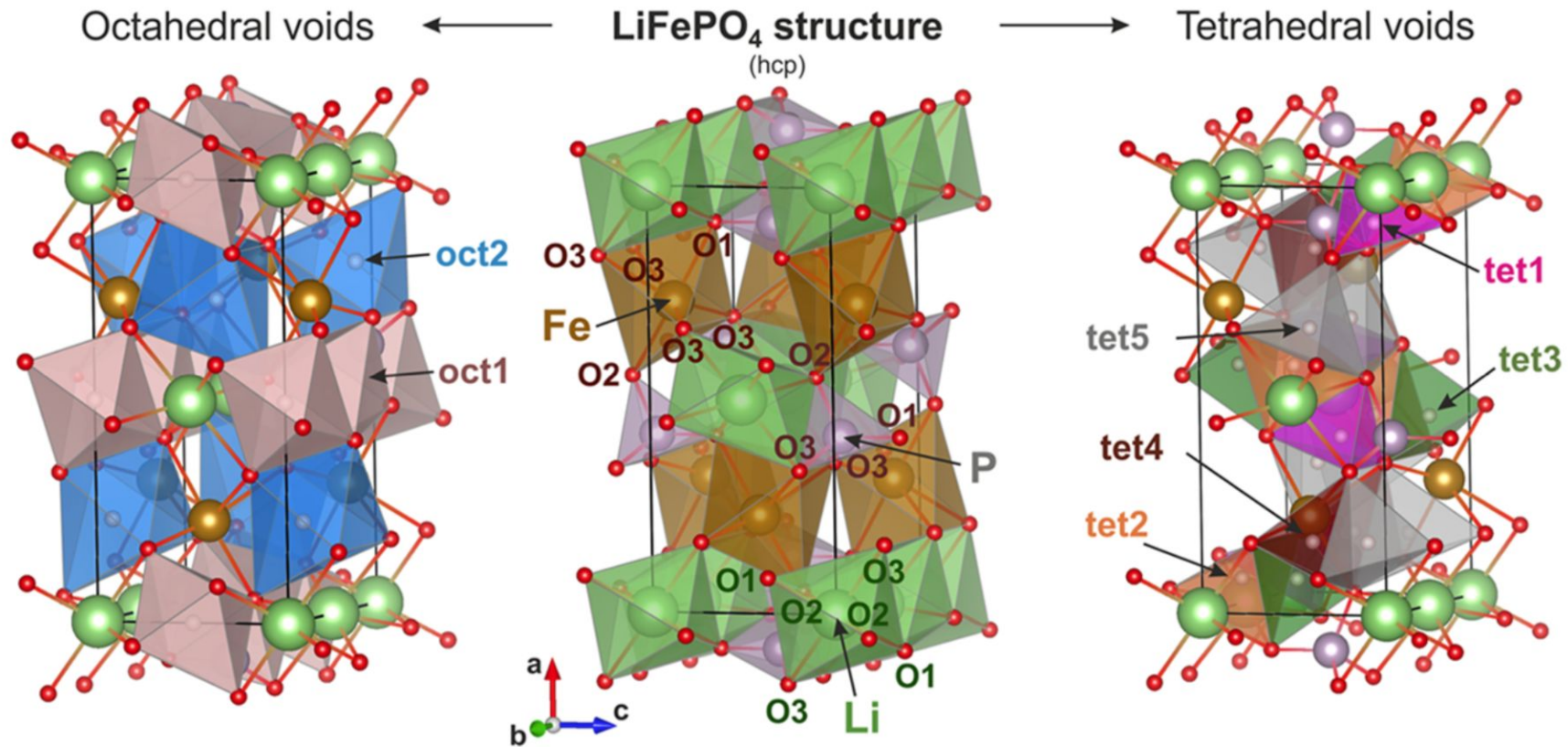
Formation energy of P vacancies

$$dE = [E(LiFeP_{1-x}Vac_xO_4) - E(LiFePO_4) + x\mu(P)]/x$$



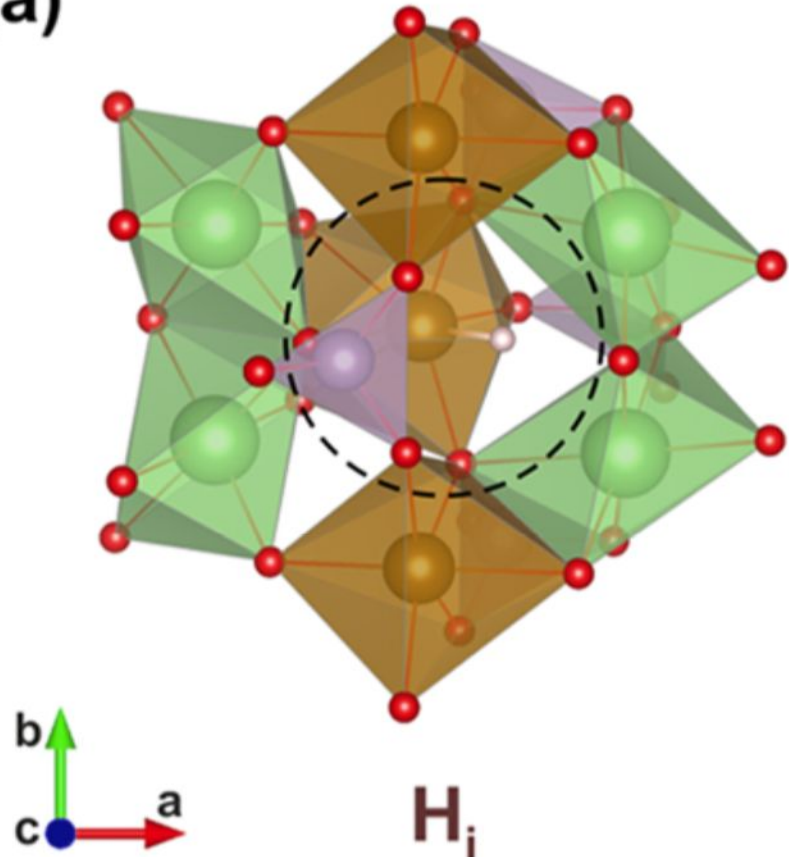
$$C_{vac} = \exp(-3.5/kT) \sim 10^{-36} \text{ at } T = 473 \text{ K} - \text{no vacancies are possible}$$

2 Octahedral and 5 tetrahedral Interstitial sites



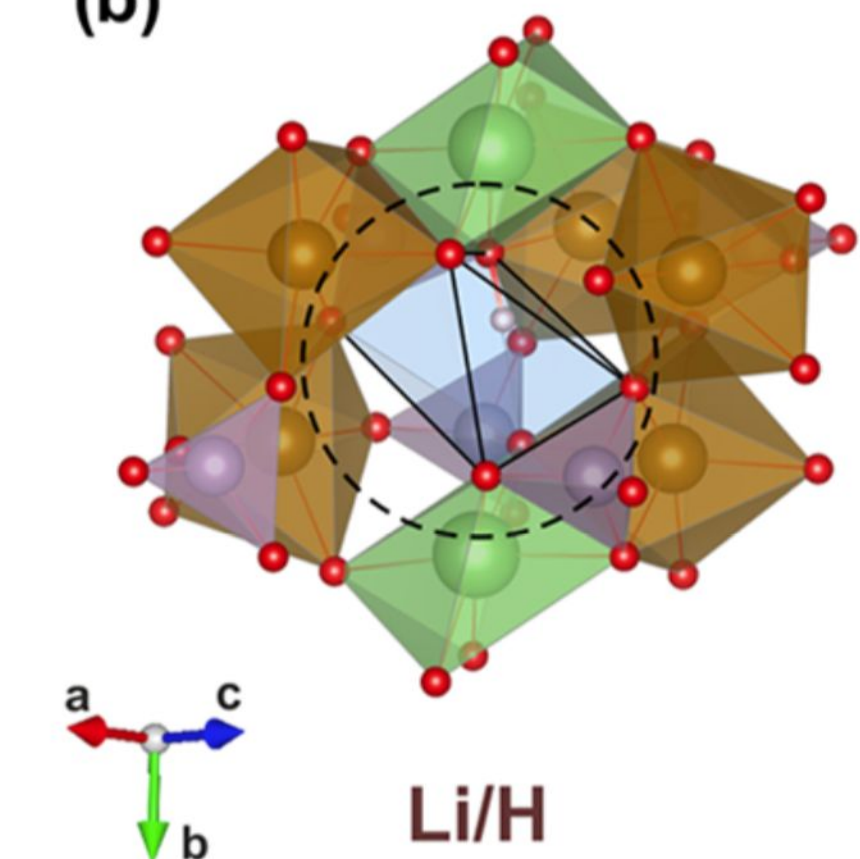
Interstitial and substitution of Li

(a)



$$E_{\text{sol}} = 3.1 \text{ eV}$$

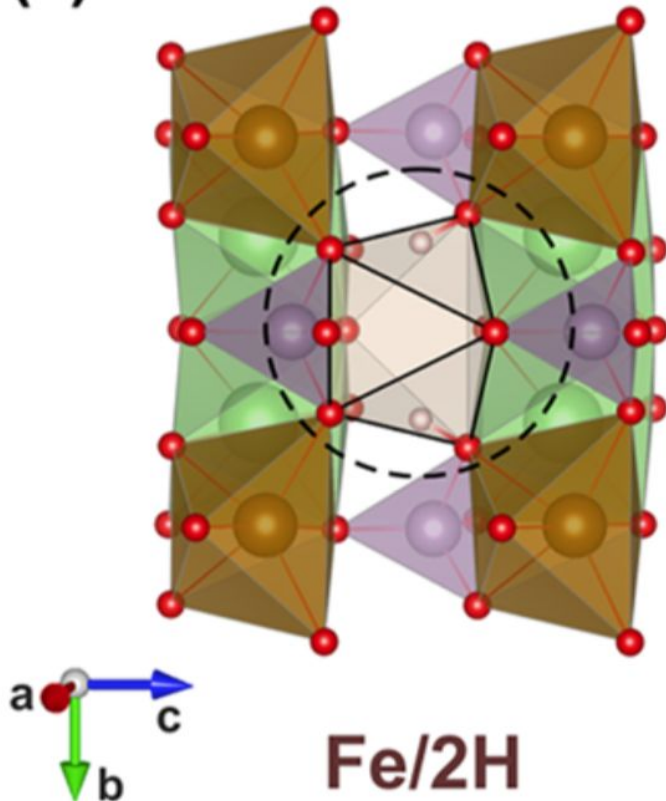
(b)



$$E_{\text{sub}} = 0.9 \text{ eV/atom } H$$

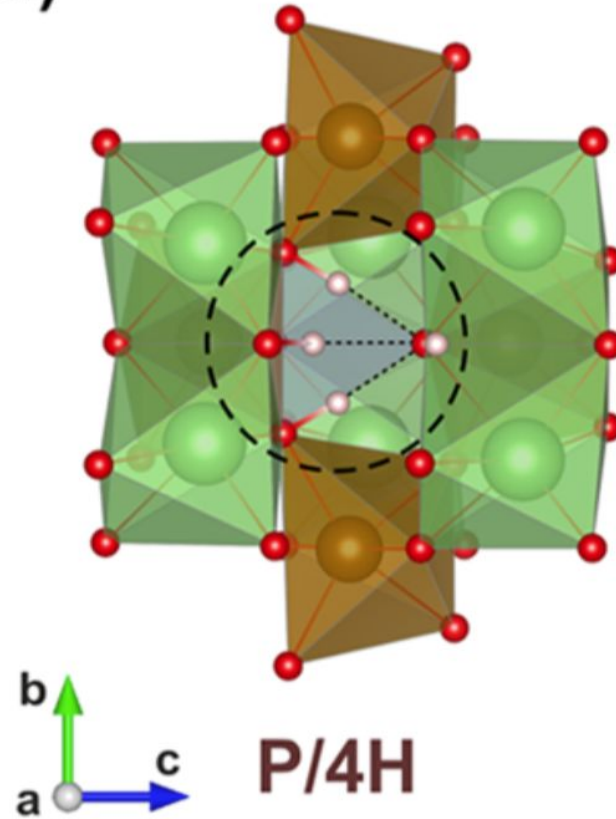
Substitution of Fe by 2H and P by 4H

(c)



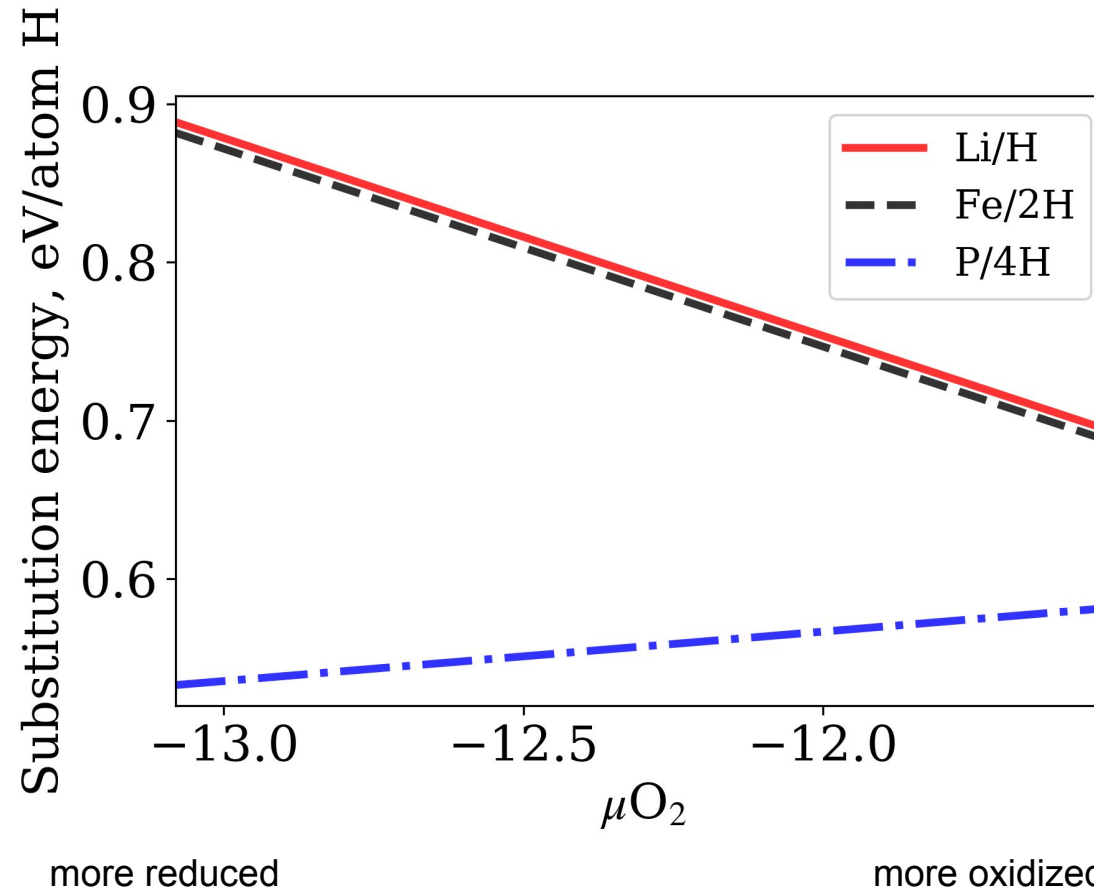
$$E_{\text{sub}} = 0.9 \text{ eV/atom H}$$

(d)



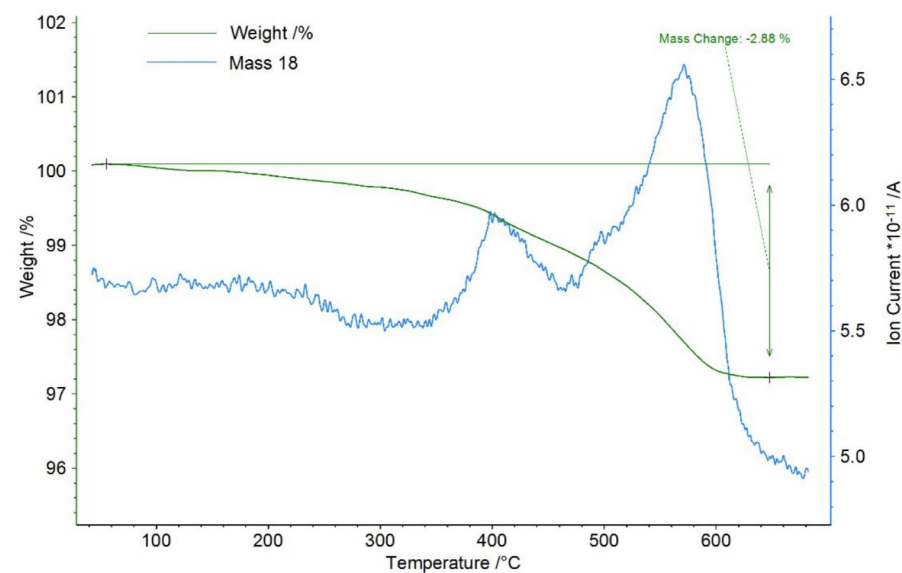
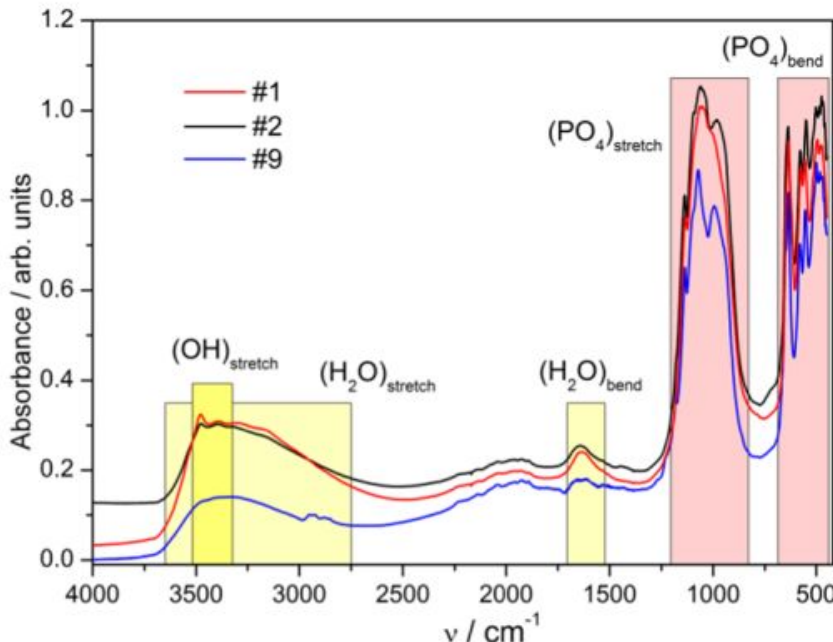
$$E_{\text{sub}} = 0.51 \text{ eV/atom H}$$

Substitution energy as a function of oxygen chemical potential



Aksyonov D.A//Inorg. Chem. 2021, 60, 8, 5497–5506

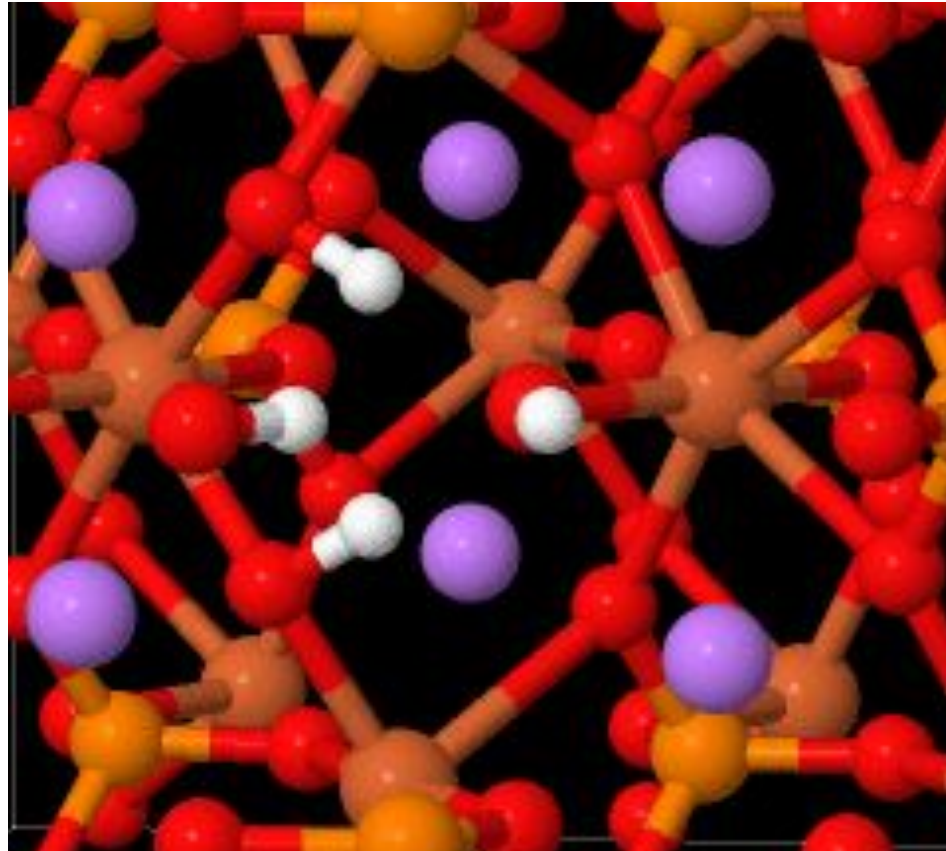
Experimental confirmation of bound OH in LiFePO₄



- However, the experimental refinement crystal structure with OH was not successful
- which is apparently caused by the disordered nature of defects
- therefore, to understand this disordering an ab initio an MD study was performed and deuterium-enriched LFP was synthesized

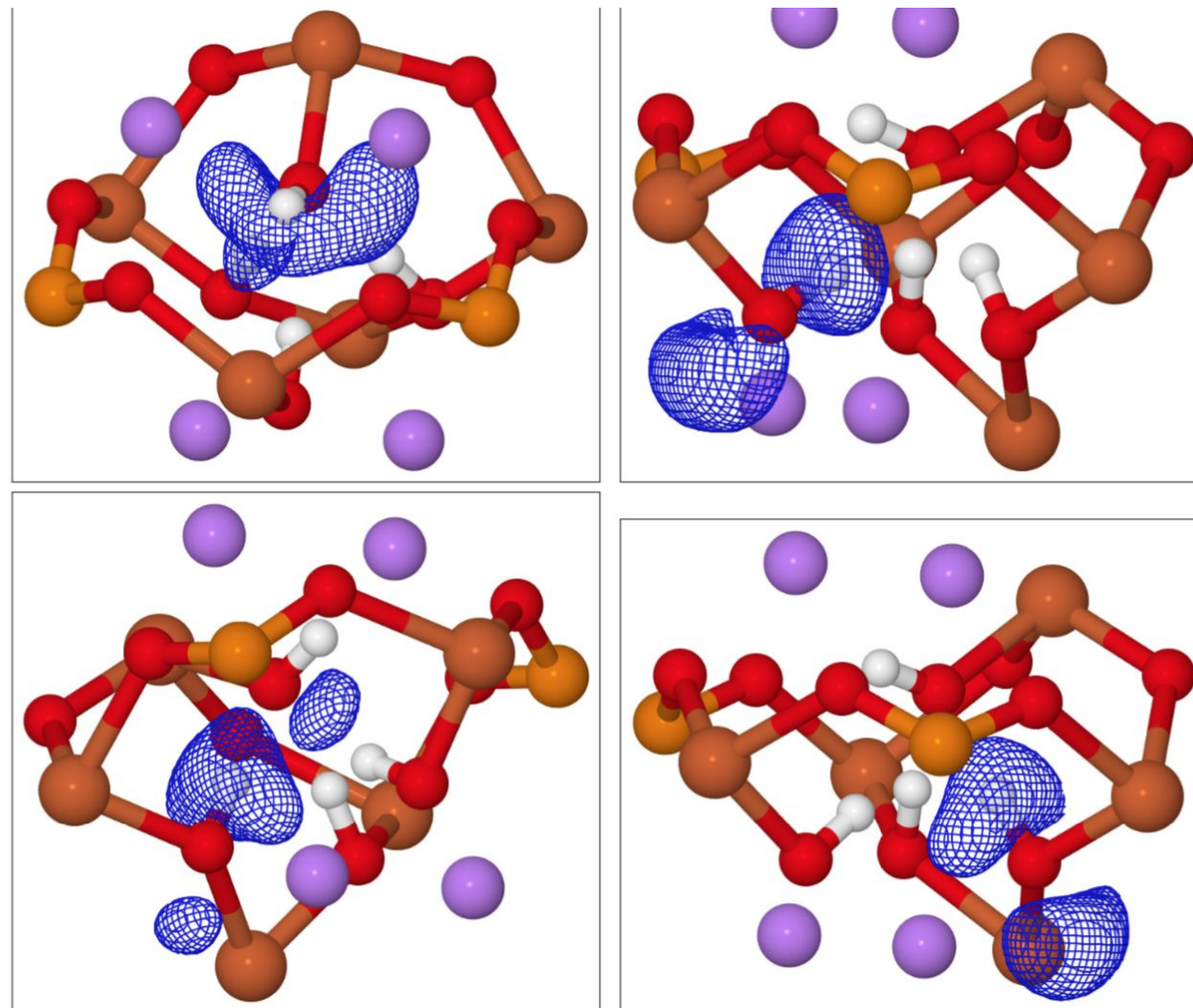
Sumanov, V D., D.A. Aksyonov, O.A. Drozhzhin, et al. // *Chemistry of Materials* 31, no. 14 (2019): 5035-5046.

Study of OH dynamics in P/4H from DFT MD

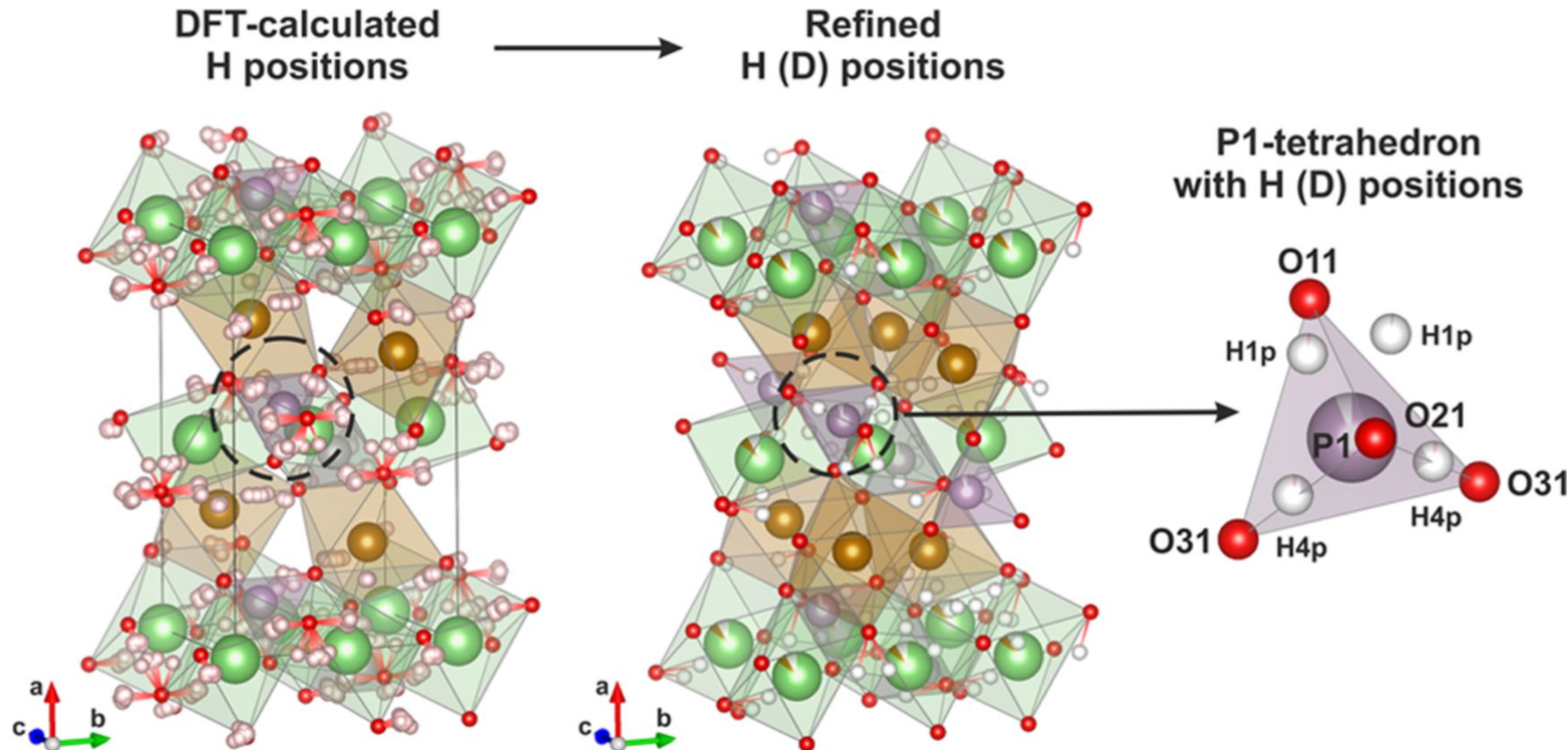


900 K, 10 ps x 10

Spatial distribution of H from MD study (P/4H)



Scheme of H occupancy refinement



Rietveld refinement with fixed H positions from DFT

Atom	<i>x</i>	<i>y</i>	<i>z</i>	Occupancy	$U_{eq}, \text{ \AA}^2$
Li11(M1)	0	-0.25	-0.25	0.855(13)	0.0073(6)
Fe11(M1)				0.066(2)	
Fe21(M2)	0.2996(15)	0	0.7221(17)	1.000(3)	0.0091(5)
Li21(M2)				0.000(15)	
Fe22(M2)	-0.2634(15)	-0.5	-0.2300(17)	1.000(3)	0.0091(5)
Li22(M2)				0.000(15)	

P11

P12

O11

O12

O21

O22

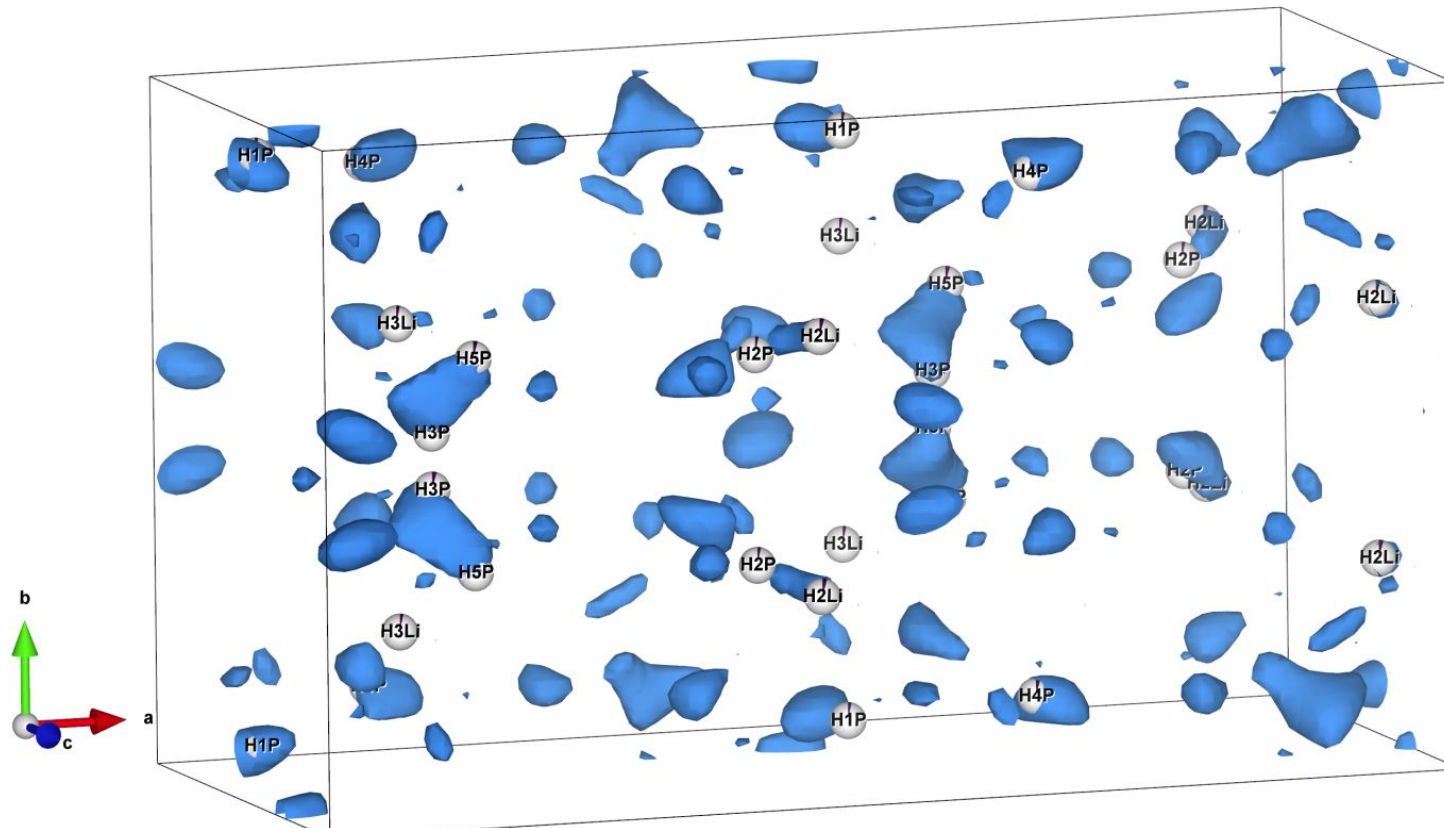
3.2 wt. % from refinement

vs

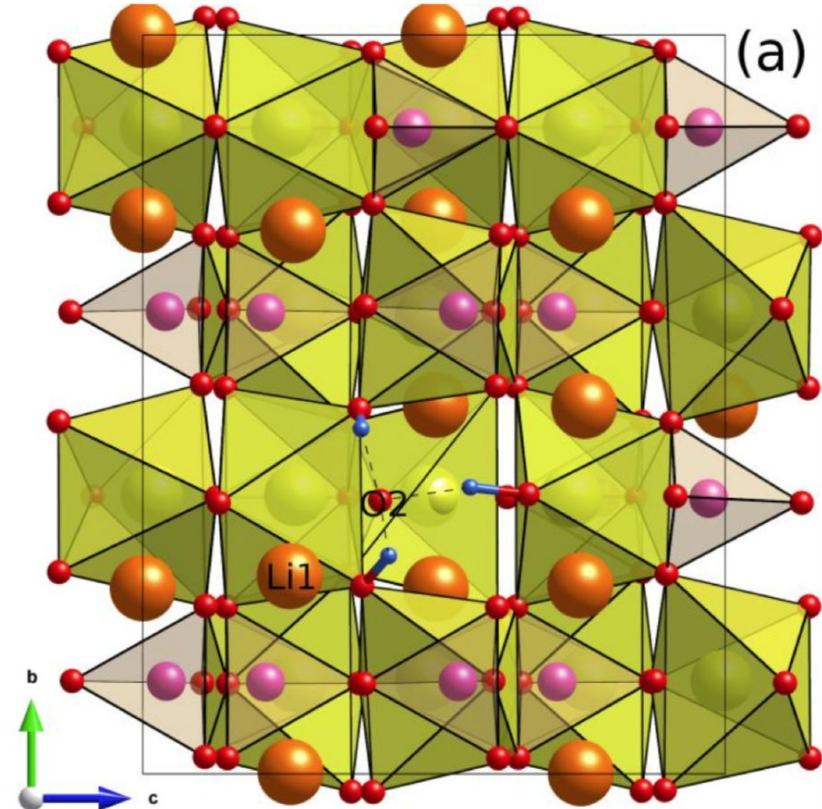
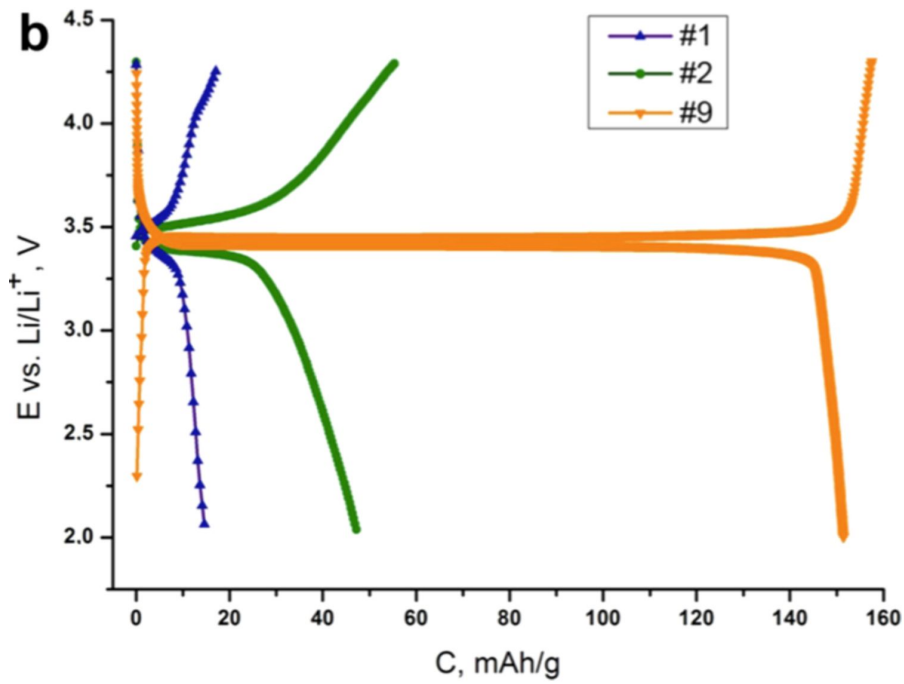
2.9 wt. % from TGA

O31	0.1874(15)	-0.2037(12)	0.0580(12)	1	0.0101(4)
O32	-0.1442(15)	-0.2957(12)	-0.5285(12)	1	0.0101(4)
H1P	0.02544	-0.07054	0.43917	0.034(6)	0.04
H2P	0.89517	0.34678	0.09716	0.032(6)	0.04
H3P	0.14099	0.45871	0.6883	0.041(4)	0.04
H4P	0.15584	0.88144	0.20274	0.045(5)	0.04
H5P	0.16603	0.34451	0.77051	0.039(4)	0.04
H1Li	0.55243	0.68796	0.44661	0.018(5)	0.04
H2Li	0.4335	0.31065	0.02674	0.045(5)	0.04
H3Li	0.58568	0.27569	0.144	0.031(7)	0.04

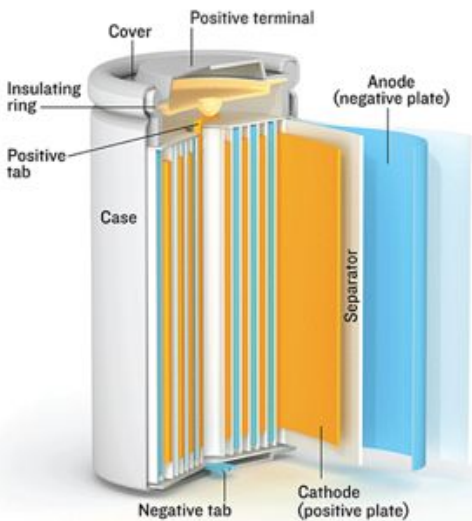
Difference Fourier map for LFP structure refined without hydrogen and DFT predicted positions



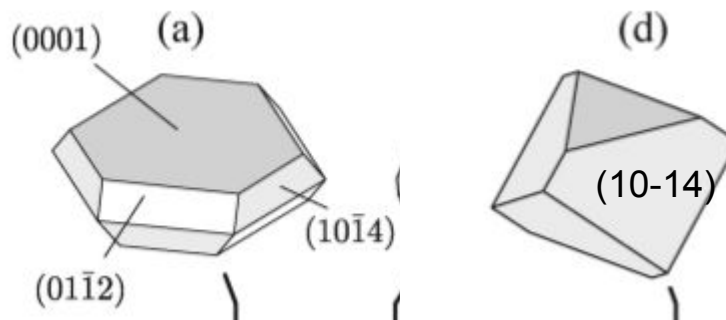
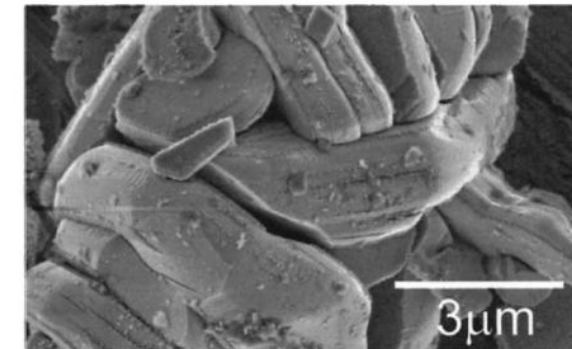
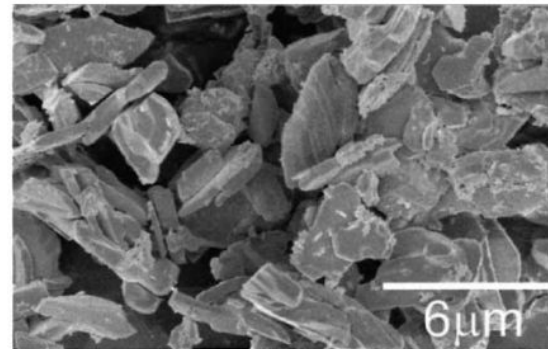
Practical implications



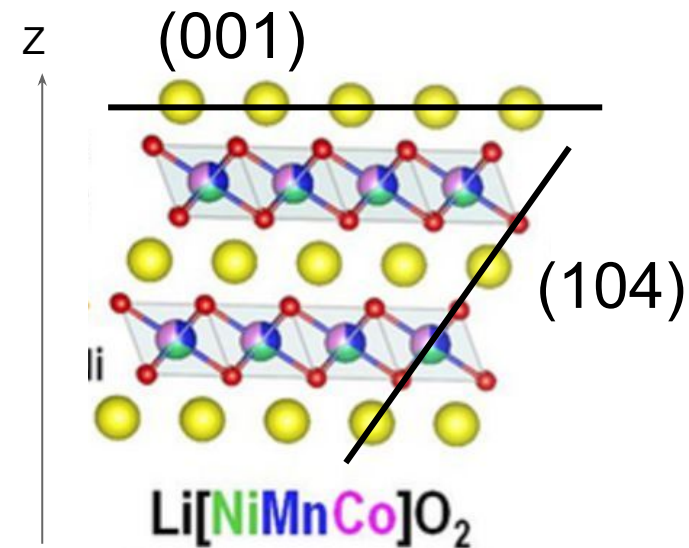
Morphology and surface structure of cathode particles is highly important!



(b) O₂-LiCoO₂

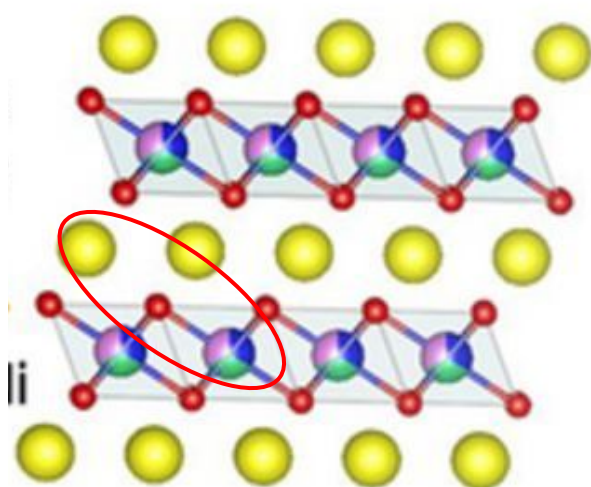


Carlier2001 Kramer2009

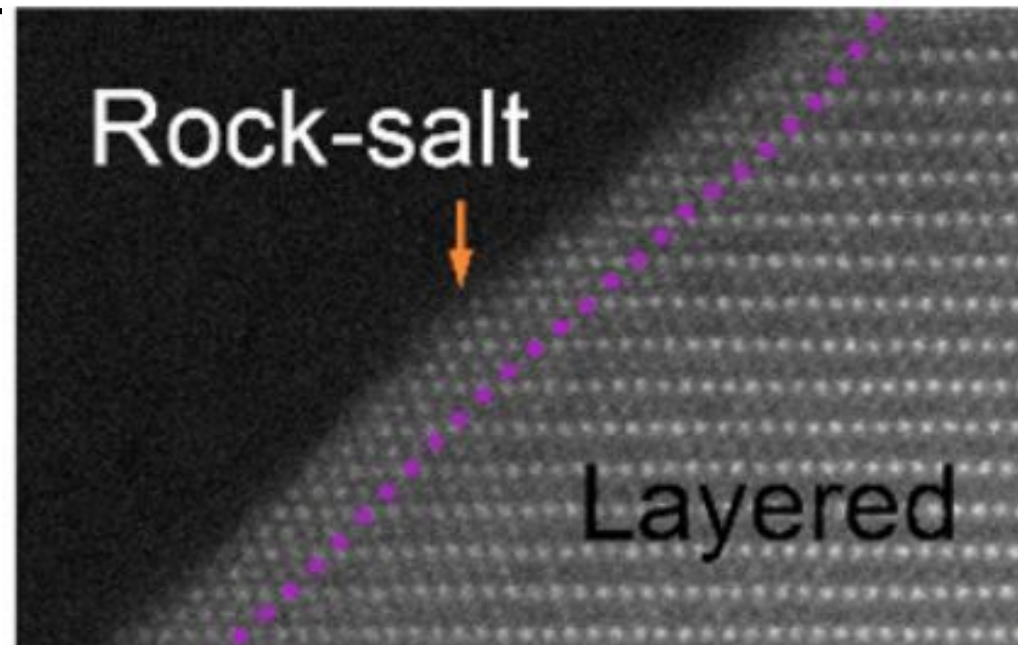


What happens on the surface?

Rocksalt-type surface reconstruction



TEM of (104)
Li[NiMnCo]O₂



(104)hex -> (002)cubic

Zhang2018

Main question

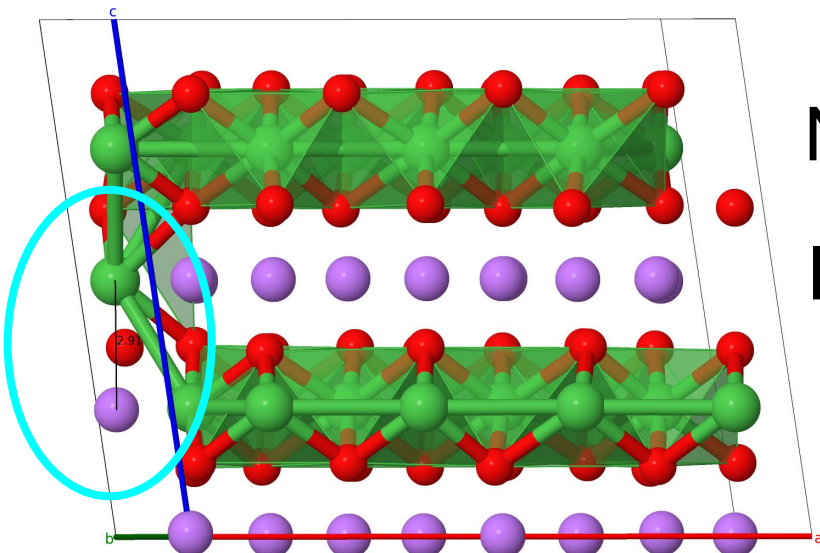
Is surface reconstruction based on antisite pairs kinetically controlled or any thermodynamic driving force exists?



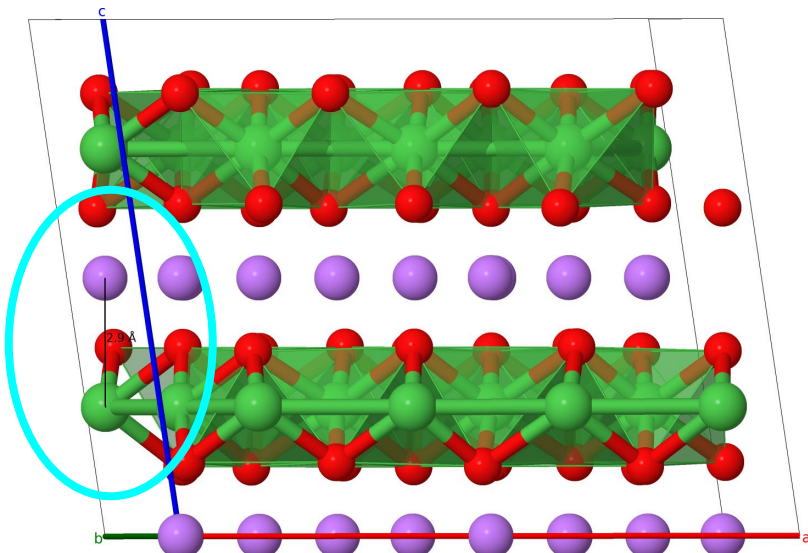
Make DFT+U atomic simulation neglecting the influence of electrolyte.

Formation energy of antisites

Very important type of defects in layered oxides, up to 10% in LiNiO_2 , but much smaller in LiCoO_2



Ni
Li



$$\Delta E_{\text{AS}} = E(\text{supercell with antisite}) - E(\text{ideal supercell})$$

Antisite pairs formation energies

Phase	space group	AS energy
LiNiO_2	$R-3m$	-0.8 eV
LiCoO_2	$R-3m$	1.9 eV
NaNiO_2	$C2/m$	2.1 eV
NaCoO_2	$R-3m$	2.9 eV

Negative antisite formation energy for LiNiO_2 !

May be the problem with LiNiO_2 space group?

- LiNiO_2 is often reported in **R-3m** group, where all Ni-O bonds are fixed to 1.99 Å.
- However Jahn-Teller (**JT**) distortion and charge ordering of Ni^{3+} to Ni^{2+} and Ni^{4+} are possible with the reduction of energy

LiNiO_2 in $P2/c$ with charge order is most stable

PHYSICAL REVIEW B 84, 085108 (2011)

Charge disproportionation and Jahn-Teller distortion in LiNiO_2 and NaNiO_2 : A density functional theory study

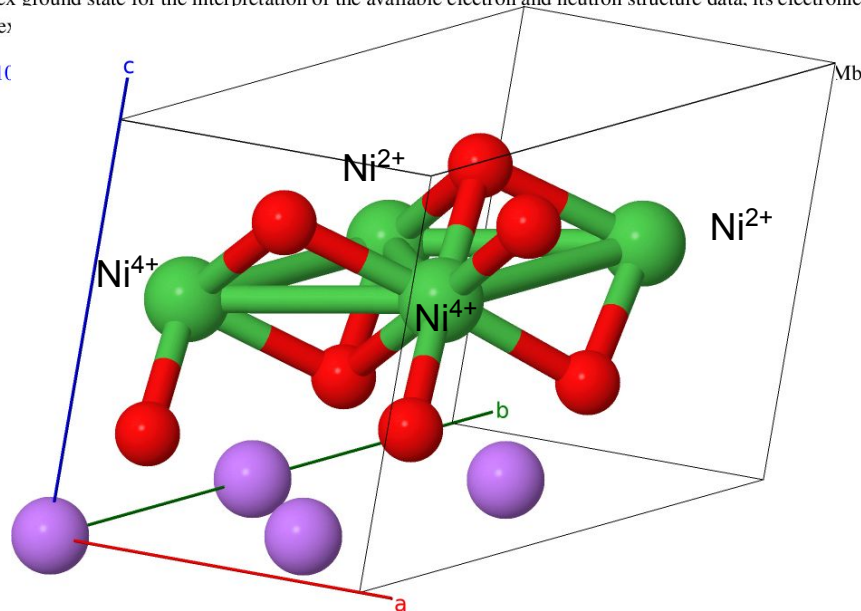
Hungru Chen,* Colin L. Freeman, and John H. Harding

Department of Materials Science and Engineering, University of Sheffield, S1 3JD, United Kingdom

(Received 24 March 2011; revised manuscript received 12 July 2011; published 19 August 2011)

Density functional theory calculations have been performed on three potential ground-state configurations of LiNiO_2 and NaNiO_2 . These calculations show that, whereas NaNiO_2 shows the expected cooperative Jahn-Teller distortion (and therefore a crystal structure with $C2/m$ symmetry), LiNiO_2 shows at least two possible crystal structures very close in energy (within 3 meV/formula unit): $P2_1/c$ and $P2/c$. Moreover, one of them ($P2/c$) shows charge disproportionation of the (expected) Ni^{3+} cations into Ni^{2+} and Ni^{4+} . We discuss the implications of this complex ground state for the interpretation of the available electron and neutron structure data, its electronic and comple

DOI: 10.1103



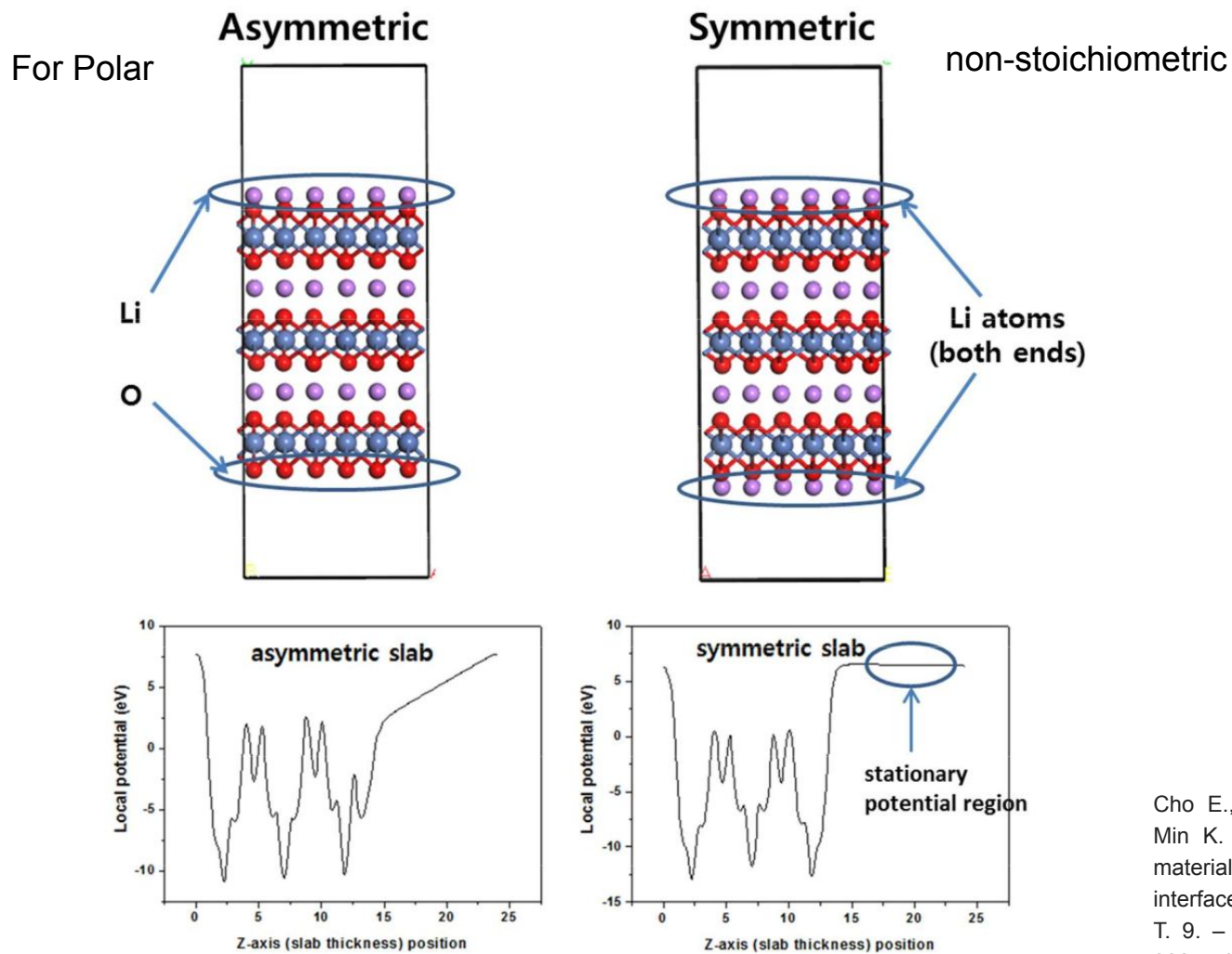
- Charge-disproportionation of Ni^{3+} to Ni^{2+} and Ni^{4+}
- According to our results the total energy reduced by 15 meV/atom
- 1.5 eV for 100-atom cell!

Antisite pairs formation energies

Phase	space group	AS energy	NN, sep, A
LiNiO_2	P2/c	0.73 eV (0.75 [1])	1nn, 2.86 Å
LiCoO_2	R-3m	1.9 eV	1nn, 2.82 Å
NaNiO_2	C2/m	2.1 eV	2nn, 4.17 Å
NaCoO_2	R-3m	2.9 eV	2nn, 4.22 Å

Chen, Hungru, James A. Dawson, and John H. Harding. "Effects of cationic substitution on structural defects in layered cathode materials LiNiO_2 ." *Journal of Materials Chemistry A* 2, no. 21 (2014): 7988-7996.

Surface energy calculations



Cho E., Seo S. W.,
Min K. ACS applied
materials &
interfaces. – 2017. –
T. 9. – №. 38. – C.
33257-33266./SI

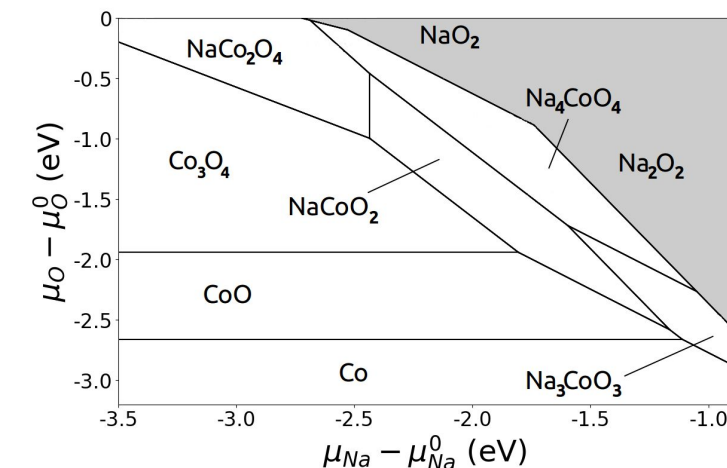
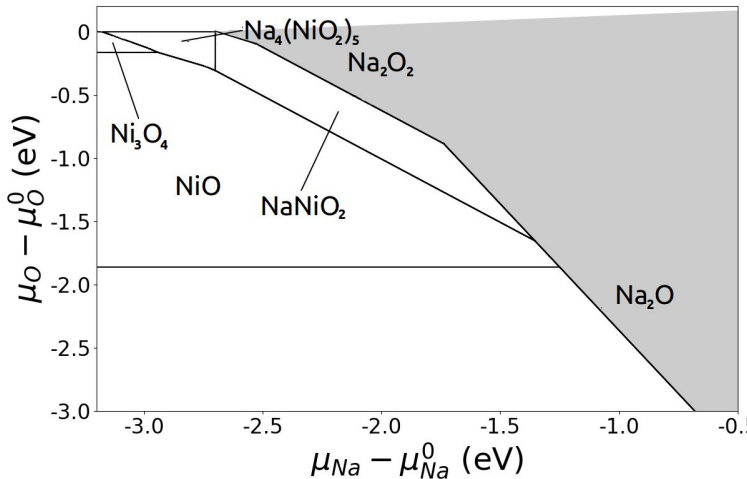
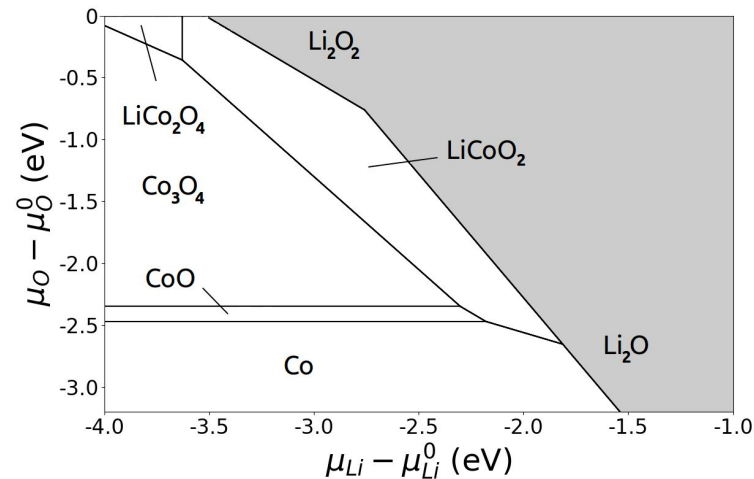
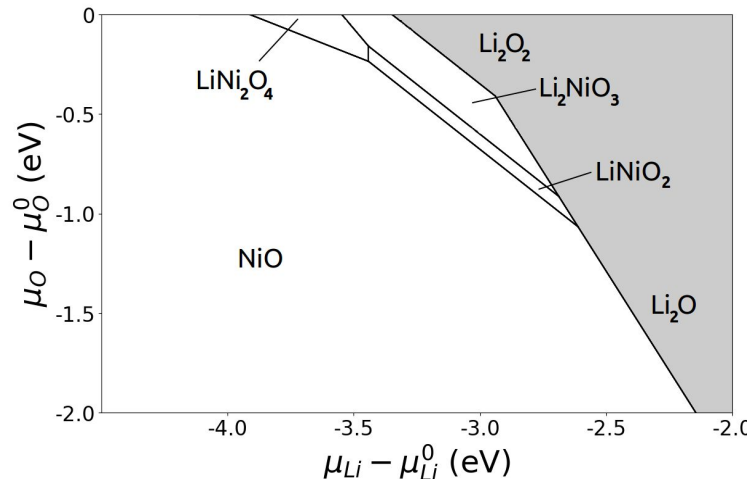
Surface energies

$$\gamma = \frac{1}{2 \cdot A} \left[E_{\text{slab}} - N_{\text{Co}} \left(\varepsilon_b - \sum_i \Gamma_i \cdot \mu_i \right) \right]$$

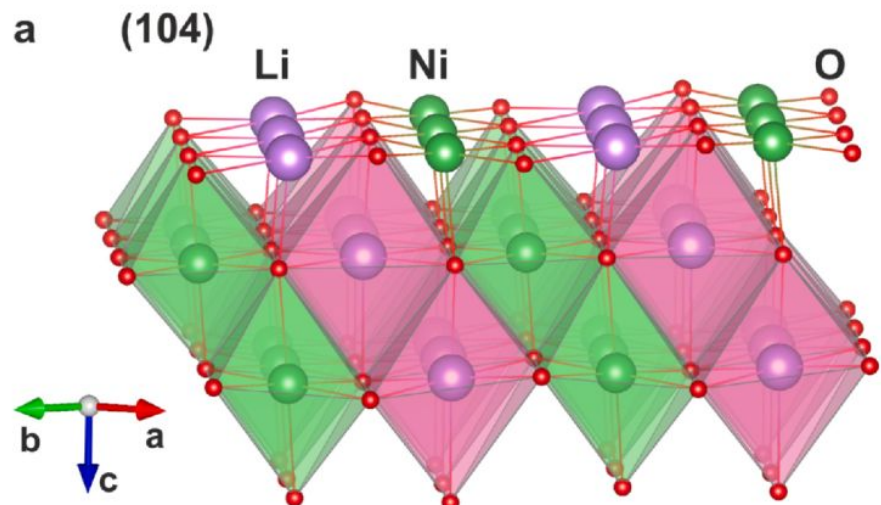
ε_b is energy of bulk cell, Γ_i is excess of i atoms in the slab

Dependence on chemical potential !
phase diagram is required

Phase diagrams in chemical potential space

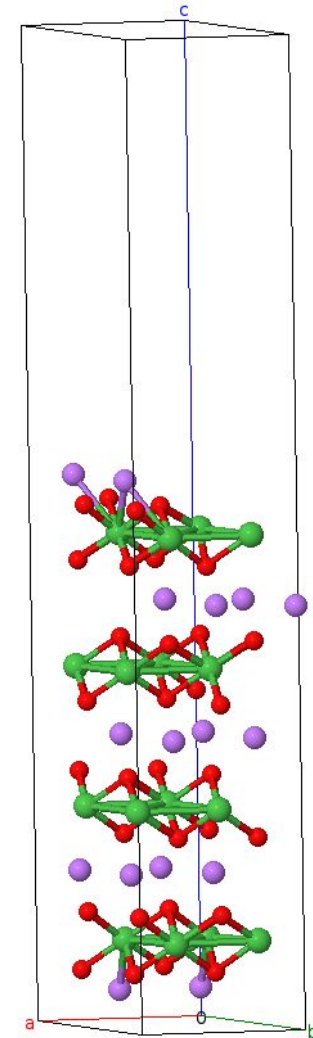


Surface structure



SIMAN: creating slabs with surfaces

```
1 st = create_surface2(sc, [0, 0, 1],  
                      cut_thickness = 10, min_vacuum_size = 10,  
                      symmetrize = 0, min_slab_size = 16)
```



Surface energy (J/m^2) of considered oxides

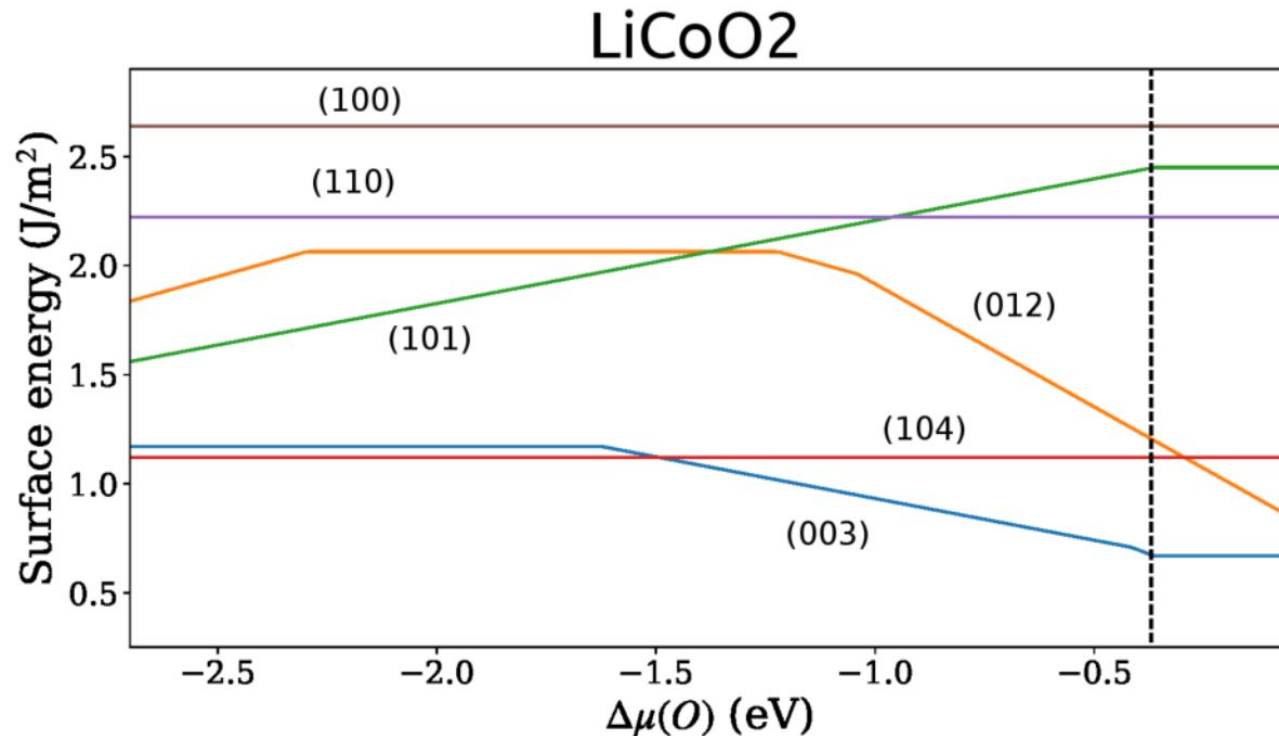
Surface	LiNiO_2 ($R-3m$)	LiCoO_2 ($R-3m$)	NaNiO_2 ($C2/m$)	NaCoO_2 ($R-3m$)
(001) $\frac{1}{2}$ ML	0.65	1.2	1.35	1.35
(104)/ (10-1)	0.55	1.1	0.35	0.87

- Surface energy correlates with number of broken bonds
- Polar surfaces have higher energy than non-polar

Considered surfaces, example of LiCoO_2

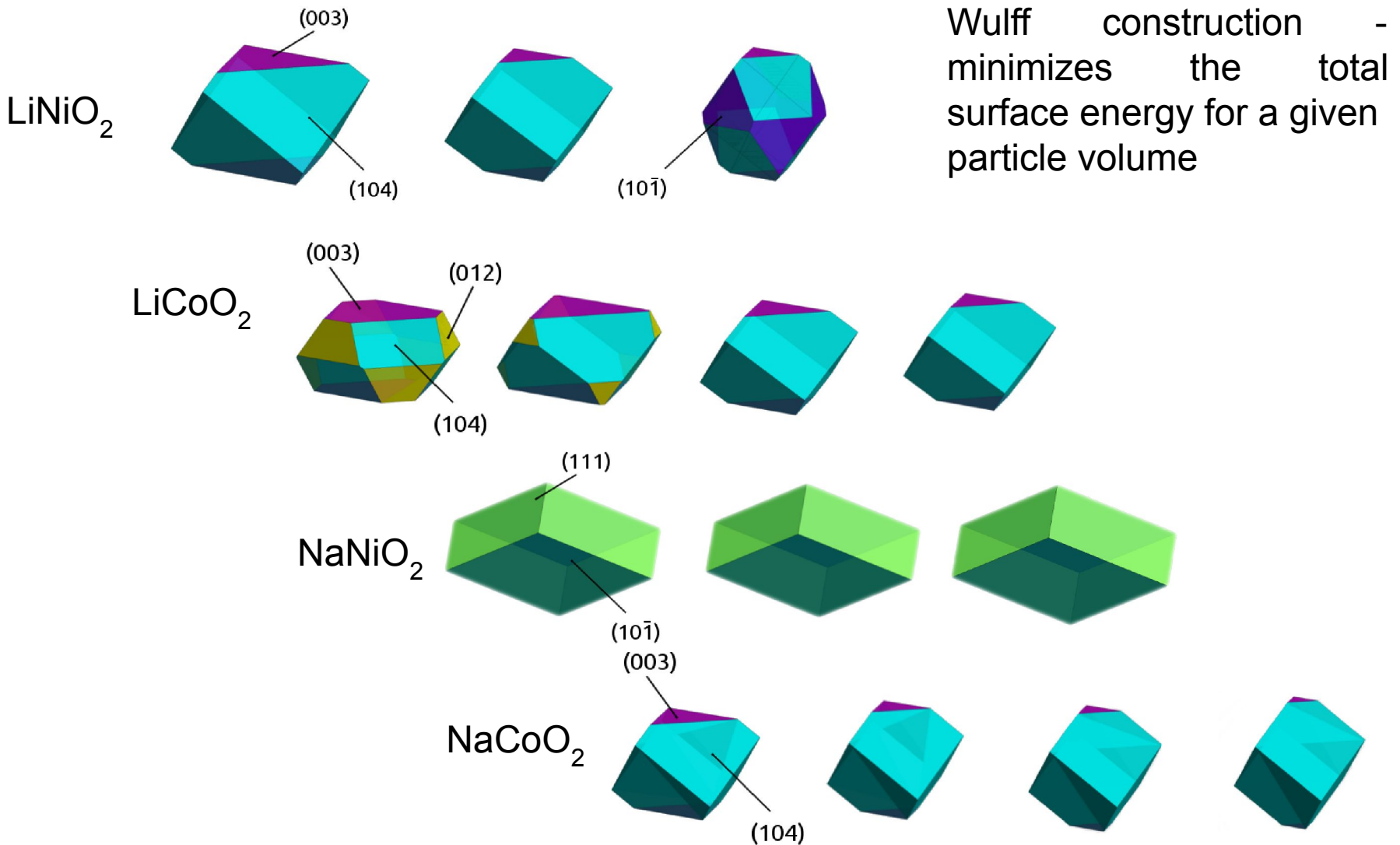
$R-3m$: non-polar (104), (110), (100), polar: (012), (003), (101), (111)

$C2/m$: non-polar (104), (10-1), (100), (111), (10-2); polar: (003), (012), (110)



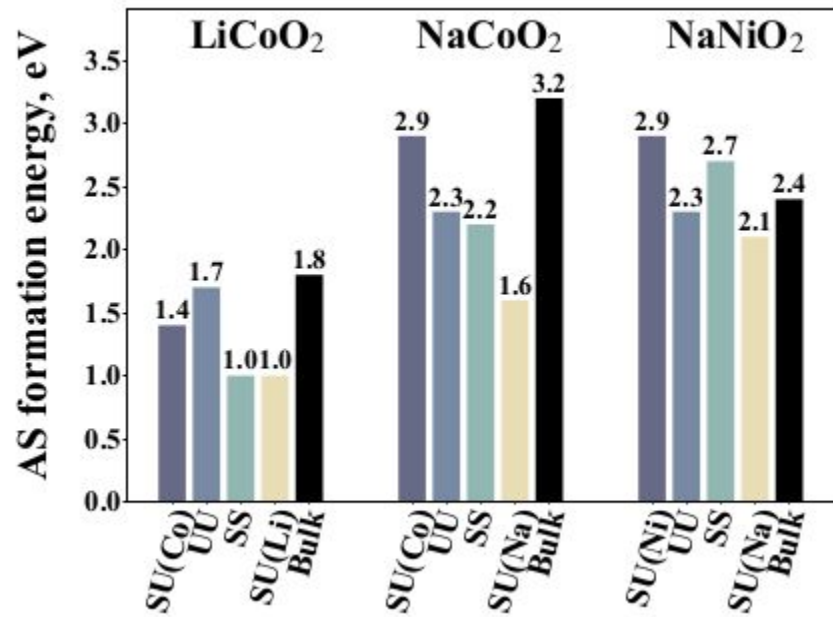
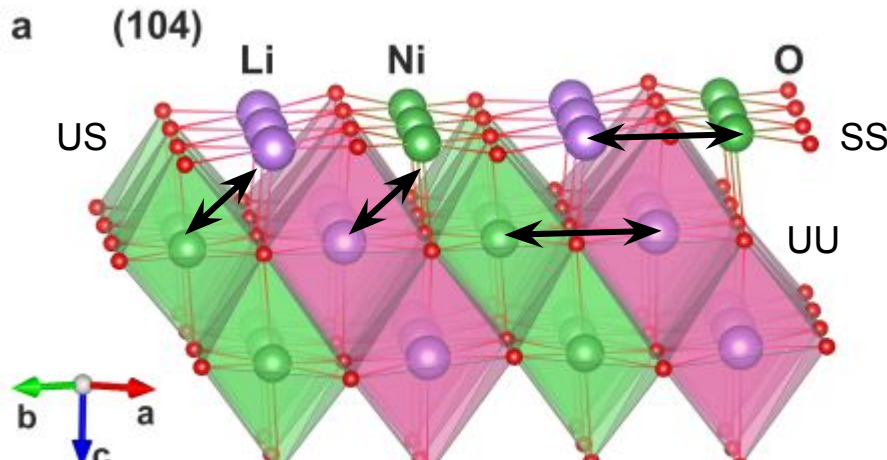
Surface energy as a function of chemical potential

Wulff construction depending on chemical potential



Wulff construction - minimizes the total surface energy for a given particle volume

Surface antisites



In Co-based oxides surface antisite pair is formed more easily, however the energy is still positive

- Influence of electrolyte?
- Kinetic control?
- Chemical composition change?

Acknowledgments



Dr. A.Boev,
Skoltech



Dr. S.Fedotov,
Skoltech



**Prof.
A. Zhugayevych**



**Prof.
K.Stevenson,**



**Prof.
A.Abakumov,**
Skoltech

O.A. Drozhzhin
E.V. Antipov

Thank you for your attention!